Fisheries New Zealand

Tini a Tangaroa

Acoustic survey of spawning hoki in Cook Strait and off the east coast South Island during winter 2019

New Zealand Fisheries Assessment Report 2020/21

R.L. O'Driscoll,
P. Escobar-Flores

ISSN 1179-5352 (online)
ISBN 978-1-99-002585-3 (online)

August 2020

New Zealand Government

Requests for further copies should be directed to:

Publications Logistics Officer
Ministry for Primary Industries
PO Box 2526
WELLINGTON 6140

Email: brand@mpi.govt.nz
Telephone: 0800 00 83 33
Facsimile: 04-894 0300

This publication is also available on the Ministry for Primary Industries websites at:
http://www.mpi.govt.nz/news-and-resources/publications
http://fs.fish.govt.nz go to Document library/Research reports

TABLE OF CONTENTS

EXECUTIVE SUMMARY

O'Driscoll, R.L; Escobar-Flores, P. (2020). Acoustic survey of spawning hoki in Cook Strait and off the east coast South Island during winter 2019.

***New Zealand Fisheries Assessment Report 2020/21.* 50 p.**

The 21st acoustic survey of spawning hoki (*Macruronus novaezelandiae*) abundance in Cook Strait was carried out using the research vessel *Kaharoa* from 17 July to 28 August 2019 (voyage code KAH1904). Seven acoustic snapshots of the main Cook Strait spawning grounds were completed with good coverage of the spawning season. The acoustic survey also included the other major eastern spawning areas off the east coast South Island (ECSI), with two snapshots of Pegasus Canyon and one of Conway Trough. The acoustic work was supported by 11 trawls in Cook Strait and 3 trawls in Pegasus Canyon for mark identification and collection of biological samples. Four attempts were made to collect *in situ* data on tilt angle distributions of hoki in Cook Strait using lowered cameras.

The acoustic abundance index for Cook Strait in 2019 was 91 000 t, which was 11% lower than the equivalent index from the 2017 survey (102 000 t), and the lowest since 2008. The model weighting (expressed as a coefficient of variation, CV), which includes uncertainty associated with survey timing, sampling precision, acoustic detectability, mark identification, calibration, and target strength, was 36%. Hoki abundance in Cook Strait from individual snapshots ranged from 46 000 t (on 18–19 August) to 124 000 t (on 18–19 and 29–30 July). As in previous surveys, most of the hoki backscatter was concentrated in Cook Strait Canyon, but aggregations were also observed in the Narrows Basin and in Nicholson Canyon. Aggregations of hoki also occurred in Pegasus Canyon, with an average acoustic abundance estimates of 55 000 t from two snapshots of this area on 15–16 August. The single snapshot of Conway Trough on 17 August had an estimated biomass of 15 000 t. About 53% of the hoki biomass in Cook Strait and 64% of the biomass in Pegasus Canyon came from hoki schools. No hoki schools were observed in Conway Trough.

1. INTRODUCTION

Hoki (*Macruronus novaezelandiae*) is New Zealand's largest finfish fishery with a TACC of 150 000 t in 2018–19 (although 20 000 t was ‘shelved’ by industry agreement), reducing to 115 000 t from 1 October 2019. Although managed within a single quota management area (QMA), hoki are assessed as two stocks, western and eastern. Juveniles from both stocks mix on the Chatham Rise and recruit to their respective stocks as they approach sexual maturity. Spawning occurs in winter (June to September), with the major spawning areas off the west coast of the South Island (WCSI) for the western stock, and in Cook Strait for the eastern stock.

On the spawning grounds, hoki typically form large midwater aggregations. The occurrence of readily identifiable, single-species aggregations clear of the seabed allows for accurate abundance estimation using acoustics. Acoustic surveys of spawning hoki have been conducted regularly since a 1984 pilot survey of the WCSI spawning grounds (Coombs & Cordue 1995). The results of acoustic surveys of spawning hoki in Cook Strait and the WCSI have been important inputs into hoki stock assessments for over 25 years

Acoustic surveys of hoki spawning grounds in Cook Strait were carried out on research vessels annually from 1991–2008, except 2000, 2004, and 2007. Since 2007, industry vessels have also surveyed part of Cook Strait during the hoki spawning season using the same (NIWA-established) protocols as for the prior research vessel surveys (O’Driscoll & Dunford 2008, O’Driscoll & Macaulay 2009, 2010, O’Driscoll 2012, O’Driscoll et al. 2015, 2016). In 2017, no suitable industry vessel was available, and acoustic data collection was carried out from the NIWA coastal research vessel *Ikatere* (O’Driscoll & Escobar-Flores 2018), meaning no mark-identification trawling was carried out that year.

The Medium-Term Research Plan for Deepwater Fisheries includes acoustic surveys of the Cook Strait hoki spawning grounds every two years to update the abundance indices. Although the acoustic results from Cook Strait have not been very influential on the results of the stock assessment model (e.g., McKenzie 2018), it is considered necessary to monitor the abundance of the eastern spawning stock independently of the Chatham Rise, where both eastern and western hoki are mixed together.

Because no suitable industry vessel was available in 2019, the main fishing grounds in Cook Strait were surveyed during the spawning season using the NIWA research vessel *Kaharoa* to carry out acoustic data acquisition and mark-identification trawling over a 42-day period from 17 July–28 August 2019 (Figure 1).

Eastern hoki also spawn off the east coast of the South Island (ECSI) in an area centred on Pegasus Canyon (Figure 2), north of Banks Peninsula (Livingston 1990). Annual catches of 2800–4400 t have been taken from this area in the last 5 years (Fisheries New Zealand 2019). Two acoustic surveys of Pegasus Canyon were carried out from a commercial vessel in 2002 and 2003 (O’Driscoll 2003, O’Driscoll et al. 2004). These surveys confirmed that the ECSI is a significant satellite spawning area for the eastern hoki stock, with acoustic biomass estimates from Pegasus Canyon being 35 and 43% of the equivalent estimates from Cook Strait in 2002 and 2003 respectively. Acoustic surveys of Pegasus Canyon were also completed during the 2006 and 2008 research voyages on *Kaharoa* (O’Driscoll 2007, 2009), and during the 2013 voyage from *Thomas Harrison* (O’Driscoll et al. 2015). These surveys showed that significant aggregations still occur in this area, with the biomass estimates for Pegasus Canyon being 24–38% of the equivalent estimates from Cook Strait. In 2019, further acoustic estimates of hoki spawning in Pegasus Canyon were obtained, to compare with the estimates from Cook Strait. The voyage also surveyed Conway Trough (Figure 2), off Kaikoura, where spawning hoki have sometimes been observed (e.g., O’Driscoll 2003, 2007, 2009, O’Driscoll et al. 2004).

Knowledge of target strength (TS) is necessary to convert the backscatter measured by acoustic surveys and attributable to hoki to produce an estimate of biomass. The relationship between TS and fish total length for hoki was revised based on TS data collected during the 2012 west coast South Island survey using an acoustic-optical system (AOS) (Dunford et al. 2015). These measurements were made on hoki being herded by a trawl, but results are dependent on statistical assumptions about the tilt angle distribution of undisturbed hoki. To investigate the validity of this assumption, and thus confirm that the AOS provides unbiased estimates of TS, we deployed an underwater camera system during the 2019 survey to attempt to measure the tilt angle distribution of hoki *in situ*.

1.1 Project objectives

This report fulfils the reporting requirements for Objectives 1 and 2 of Fisheries New Zealand Research Project HOK2019/01:

1. To continue the time series of relative abundance indices of spawning hoki in Cook Strait using acoustic surveys, with a target coefficient of variation (CV) of the estimate of 30%.

2. To provide a relative abundance index of hoki in Pegasus Canyon using acoustic surveys, with a target CV of the estimate of 30%.

2. METHODS

2.1 Survey design

Hoki have a long spawning season, from July to September. It is thought that during the spawning season there is a turnover of fish on the grounds. Therefore, there is no time at which all the spawning fish are available to be surveyed (Coombs & Cordue 1995). The survey design devised to deal with this problem consists of a number of subsurveys or "snapshots" spread over the spawning season. Each snapshot consists of a series of random transects (following the design of Jolly & Hampton (1990)) across strata covering the known distribution of spawning hoki. Estimates of spawning biomass are calculated for each of the snapshots and are then averaged to obtain an estimate of the "mean plateau height" (average biomass during the main spawning season). Under various assumptions about the timing and length of the spawning season (Cordue et al. 1992, Coombs & Cordue 1995), estimates of mean plateau height form a valid relative abundance time series.

In a simulation study, O'Driscoll (2004) found that the optimal survey design for Cook Strait is a long survey (more than 26 days) centred about 7 August, with at least six snapshots. This ensures that interannual variation in the timing of the season can be dealt with, as can any systematic trends in the spawning biomass through the season. Increasing the number of snapshots reduces bias and increases precision, but there is relatively little advantage in having a survey with more than six snapshots as long as those snapshots are spread over a long survey period. In 2019, the acoustic survey was carried out on *Kaharoa* from 17 July to 28 August (KAH1904). The timing and design were similar to that used successfully since 2001. However, as in 2006 and 2008, the requirement to survey other eastern spawning grounds meant that the time available to carry out snapshots of Cook Strait was reduced.

Because of the proximity of the Cook Strait spawning grounds to Wellington, *Kaharoa* made short (2–4 day) trips to the Cook Strait survey area when weather allowed. The other eastern spawning grounds are about 180–250 km from Wellington (see Figure 2) and required more extended trips. Only one trip to the ECSI spawning grounds was planned during the 2019 survey period.

The stratum boundaries and areas in Cook Strait (Figure 1, Table 1) were the same as in previous surveys, with six main strata (strata 1, 2, 3, 5A, 5B, and 6), covering the areas with depth greater than 200 m (or 180 m in stratum 2). The acoustic survey area in Cook Strait includes grounds which are not commercially fished by the fleet. For example, targeting of hoki by vessels greater than 28 m is not permitted in the Cook Strait Hoki Management Area (which mainly encompasses the Narrows Basin, stratum 1) under the industry agreed Operational Procedures for the Hoki Fishery (version 18), to reduce the catch of small hoki. In 2019, there was also a temporal closure, with the entire Cook Strait hoki seasonal spawning area (HSSA) closed between 0000 NZST on 1 August and 2400 NZST on 7 August.

The stratum boundaries and areas in Pegasus Canyon and Conway Trough (Figure 2, Table 1) were based on the survey in 2003 from an industry vessel (O'Driscoll et al. 2004). As in Cook Strait, the strata included areas with depth greater than 200 m. Pegasus Canyon was subdivided into two strata, because the highest densities of hoki tended to occur in the southern part of the Canyon (PCB) in 2002 and 2003 (O'Driscoll 2003, O'Driscoll et al. 2004). The Pegasus hoki HSSA was closed between 0000 NZST on 1 September and 2400 NZST on 7 September 2019.

2.2 Vessels and equipment

R.V. *Kaharoa* is a 28 m stern trawler with a beam of 8.2 m, displacement of 302 t, and engine power of 522 kW. A Simrad EK60 general-purpose transceiver was installed on *Kaharoa* and connected to the hull-mounted Simrad ES38B 38-kHz transducer. The acoustic system on *Kaharoa* was calibrated in Wellington Harbour before the start of the survey on 18 July 2019 (Appendix 1). The calibration was of excellent quality and indicated that the echosounder was functioning correctly, with the estimated calibration parameters similar to those from previous calibrations.

To collect high quality acoustic data, it is necessary that the transducer lies below the surface bubble layer produced by surface waves and turbulence. *Kaharoa*'s relatively shallow draft limits the range of weather conditions in which the hull-mounted system can acquire quality data. Previous Cook Strait acoustic surveys from *Kaharoa* used towed acoustic systems to circumvent this issue (e.g., O'Driscoll 2009). However, it was not possible to use the towed system for the 2019 voyage, because the decision to use *Kaharoa* as the survey vessel was made too late to allow the associated winches and deployment/retrieval systems to be overhauled and fitted.

2.3 Acoustic data collection

Acoustic snapshots were only carried out during periods of good weather (less than 25 knots of wind and 2 m swell) to ensure high quality data, but with an aim to spread the Cook Strait snapshots at regular intervals during the survey period.

Transects were run at speeds of 8–10 knots. The acoustic survey was interrupted between transects for mark identification trawls. The aim was to complete each Cook Strait snapshot within 48 hours (preferable, 72 hours absolute maximum). All transects in the main Cook Strait Canyon (strata 5A and 2) were run sequentially (i.e., without breaks), because of fish movement related to tide in this area.

2.4 Mark identification trawling

Midwater trawls were carried out for mark identification and to collect hoki length frequency and biological data. These were mostly targeted on marks where expert estimation of the species composition was uncertain. All mark identification trawls were carried out using the *Kaharoa* hoki trawl, which can be towed either in midwater or along the bottom. The *Kaharoa* hoki trawl is a Resolution-type 4-panel net manufactured by Motueka Nets with 100 m bridles, 16 m vertical opening, and a 60 mm codend. The trawl had a panel ('window') in the codend designed to burst when catches exceeded about 1000 kg. Vee-type trawl doors with a surface area of 3 m^2 were used.

For each trawl, all items in the catch were sorted into species and weighed on Marel motion-compensating electronic scales accurate to about 0.1 kg. Where possible, fish, squid, and crustaceans were identified to species level, and other benthic fauna to family. A random sample of up to 200 hoki, and 100 individuals of other species, from every tow was measured for length. In most tows, the sex and macroscopic gonad stage of all hoki in the length sample were also determined. More detailed biological data were collected on a subsample of up to 20 hoki per trawl, and included fish length, weight, sex, gonad stage (see Appendix 2), gonad weight, and removal of otoliths. Genetic samples (fin clips) were collected from 100 hoki from each area (Cook Strait and Pegasus Canyon) and preserved in 95% ethanol.

Estimated hoki length frequencies were constructed for each stratum by using all trawls within a stratum during the period of the survey and weighting individual trawl length frequencies by the hoki catch in the trawl.

2.5 Camera deployments

The camera system used to attempt to measure the tilt angle distribution of undisturbed hoki was the NIWA ‘Scampi-cam’, which consists of a still HD-camera and flashlights that can be triggered to go off at intervals (every 45 seconds). The Scampi-cam was mounted to look out horizontally into the water instead of its usual down-looking orientation.

When a mark suggesting a hoki aggregation suitable for camera deployment was identified, the camera system was lowered into the aggregation while drifting or steaming slowly (1 knot) into the current. Use of cameras required good weather and was only attempted when an aggregation of hoki was found away from the main fishing fleet. Camera deployments were short (2–3 hours), with the reaction of the fish to the cameras and lights monitored using the hull echosounder.

2.6 Other data collection

A Seabird SM-37 Microcat CTD datalogger (serial number 2958) was mounted on the headline of the net during most trawls to collect temperature and salinity data, which were then used to estimate the acoustic absorption coefficient of sound during the survey using the formula of Doonan et al. (2003).

2.7 Acoustic data analysis

Acoustic data collected during the survey were analysed using standard echo-integration methods (Simmonds & MacLennan 2005), as implemented in NIWA’s ESP3 software package (Ladroit 2017). Echograms were visually examined, and the location of the bottom in each ping determined by a combination of an in-built bottom-echo identification algorithm and manual editing. Regions corresponding to various acoustic mark types were then identified. Marks were classified subjectively from experience based on characteristics such as shape, structure, depth, strength, etc. (O’Driscoll 2002b).

Backscatter from marks (regions) identified as hoki was then integrated to produce an estimate of acoustic density, expressed as the mean area backscattering coefficient (s_a, expressed in $m^2\ m^{-2}$, see MacLennan et al. 2002). During integration, acoustic backscatter was corrected for sound absorption by seawater.

Acoustic density was output in two ways. First, average acoustic density per transect was calculated. These values were used in abundance estimation (see section 2.8). Second, acoustic backscatter was integrated over 10-ping bins to produce a series of acoustic density data for each transect. These data series have high spatial resolution, with each transect being typically made up of 30–100 data values, each value approximately 100 m apart (corresponding to 10 pings). These data are displayed in plots showing the spatial distribution of acoustic density along each transect.

Transect acoustic density estimates were converted to hoki biomass using a ratio, *r*, of mean weight to mean backscattering cross-section (linear equivalent of target strength, TS) for hoki. The method of calculating *r* was based on that of O’Driscoll (2002a):

1. using the length frequency distribution of the commercial catch from the year of the survey;
2. using the generic length-weight regression of Francis (2003) to determine mean hoki weight (*w* in kilograms)

$$w = (4.79\times10^{-6})\ L^{2.89} \qquad (1)$$

3. using the most recent TS-length relationship for New Zealand hoki (Dunford et al. 2015):

$$TS = 24.5\ \log_{10}(TL) - 83.9 \qquad (2)$$

where *TL* is total fish length in centimetres.

2.8 Abundance estimation

Abundance estimates and variances were obtained for each stratum in each snapshot using the formulae of Jolly & Hampton (1990), as described by Coombs & Cordue (1995). Stratum estimates were combined to produce snapshot estimates, and the snapshots were averaged to obtain the abundance index for 2019.

The sampling precision of the abundance index was calculated in two ways, as described by Cordue & Ballara (2001). The first method was to average the variances from each snapshot. This method potentially underestimates the sampling variance because it accounts only for the observation error in each snapshot. The imprecision introduced by the inherent variability of the abundance in the survey area during the main spawning season is ignored. The second method assumes the snapshot abundance estimates are independent and identically distributed random variables. The sample variance of the snapshot means divided by the number of snapshots is therefore an unbiased estimator of the variance of the index (the mean of the snapshots).

2.9 Survey weighting for stock assessment

The sampling precision will greatly underestimate the overall survey variability, which also includes uncertainty in TS, calibration, and mark identification (Rose et al. 2000). The model weightings (expressed as coefficient of variation or CV) used in the hoki stock assessment model are calculated for individual surveys using a Monte Carlo procedure which incorporates these additional uncertainties (O'Driscoll 2004).

The simulation method used to combine uncertainties and estimate an overall weighting (CV) for each acoustic survey of Cook Strait was described in detail by O'Driscoll (2004) and is summarised below.

Six sources of variance are considered:

- plateau model assumptions about timing and duration of spawning and residence time
- sampling precision
- detectability
- mark identification
- fish weight and target strength
- acoustic calibration

The method has two main steps. First, a probability distribution is created for each of the variables of interest. Second, random samples from each of the probability distributions are selected and combined multiplicatively in Monte Carlo simulations of the process of acoustic abundance estimation.

In each simulation, a biomass model was constructed by randomly selecting values for each variable from the distributions given in Table 2. This model was then 'sampled' at dates equivalent to the mid-dates of each snapshot. The precision of sampling was determined by the snapshot CV, and the biomass adjusted for variability in detectability. The simulated biomass estimate in each snapshot was then split, based on the proportion of acoustic backscatter in 'school' and 'fuzz' -type marks (see section 3.3 for a list of mark categories), and mark identification uncertainties were applied to each part. The biomass estimates were recombined and calibration and TS uncertainties applied in turn. The same random value for calibration and TS was applied to all snapshots in each simulated 'survey'. Abundance estimates from all snapshot estimates from the simulated survey were averaged to produce an abundance index. This whole process was repeated 1000 times (1000 simulated surveys) and the distribution of the 1000 abundance indices was output. The overall CV was the standard deviation of the 1000 abundance (mean biomass) indices divided by their mean.

3. RESULTS

3.1 2019 commercial fishery

3.1.1 Cook Strait

A total catch of 19 122 t was taken by the commercial fishery from Cook Strait between 1 June and 30 September 2019, with most hoki caught between 25 June and 15 September (Figure 3). Effort was restricted during the closure of the Cook Strait HSSA from 1 August to 7 August and no catch was taken within this period (Figure 3). The acoustic survey was within the period of high catches. Almost all the commercial effort in 2019 was concentrated in Cook Strait Canyon (strata 2 and 5A), but hoki were also caught in Nicholson Canyon (stratum 3) and in the deepwater (stratum 5B) (Figure 4).

The hoki length frequency distribution from the 2019 commercial fishery in Cook Strait (based on scientific observer data and land-based sampling for Fisheries New Zealand projects MID2019/02 and HOK2019/02) is shown in Figure 5. The mean length of hoki was 76.5 cm. Mean weight and mean backscattering cross-section (obtained by transforming the scaled length frequency distribution in Figure 5 by equations (1) and (2) and then calculating the means of the transformed distributions) were 1.44 kg and 0.000177 m^2 (equivalent to –37.5 dB) respectively, giving a ratio, *r*, for 2019 of 8155 kg m^{-2}.

Actively spawning (ripe and running ripe) female hoki were recorded in the commercial catch throughout the period of sampling from 10 June to 11 September (Figure 6). The proportion of spawning females increased sharply from 22 July, and the proportion of spent females increased in early September (Figure 6).

3.1.2 East coast South Island

A total catch of 3659 t of hoki was taken from the ECSI between 1 June and 30 September 2019. Hoki were taken from Pegasus Canyon and also from outside the acoustic survey area, east of Pegasus Canyon and along the slope to the north (see Figure 4). There was very little effort in Conway Trough. Peak catches were in early-August, late-August, and in mid-September (see Figure 3). Effort was restricted during the closure of the Pegasus HSSA from 1 September to 7 September.

The hoki length frequency distribution from the 2019 commercial fishery on the ECSI (based on scientific observer data) is shown in Figure 5. Few hoki larger than 75 cm were taken from the ECSI, and the mean length of 65.7 cm was almost 10 cm shorter than that from Cook Strait. Mean weight and mean backscattering cross-section (obtained by transforming the scaled length frequency distribution in Figure 5 by equations (1) and (2) and then calculating the means of the transformed distributions) were 0.91 kg and 0.000120 m^2 (equivalent to –39.2 dB) respectively, giving a ratio, *r*, for 2019 of 7575 kg m^{-2}.

Hoki were sampled by observers on the ECSI from 30 July to 1 August, and then from 13 August to 24 September. Actively spawning females were recorded throughout this period, with a general increase in proportion spawning in September (Figure 6).

3.2 Data collection

3.2.1 Acoustic data

Seven acoustic snapshots of the main Cook Strait spawning grounds were carried out from 18 July to 19 August 2019 (Table 3). Only one trip to the east coast South Island was possible, during mid-August, with two snapshots of Pegasus Canyon and one of Conway Trough (Table 4).

Weather conditions were particularly good in late July, allowing four snapshots to be completed in Cook Strait during the first two weeks of the voyage. Conditions in August were more variable, with a series of weather systems passing through, but it was possible to carry out surveys between the fronts, and all objectives were successfully achieved.

3.2.2 Trawl data

Eleven hoki midwater tows were carried out for mark identification in Cook Strait and all were suitable for estimating mark composition (Figure 7). Hoki were the primary catch (Table 5). Bycatch species in Cook Strait included jack mackerels (mainly *Trachurus declivis*), spiny dogfish (*Squalus acanthias*), ling (*Genypterus blacodes*), rattails (Macrouridae), red cod (*Pseudophycis bachus*), frostfish (*Lepidopus caudatus*), and mesopelagic species. Three mark-identification trawls were carried out in Pegasus Canyon (Figure 7, Table 5). One tow on a hoki school had a high catch rate of spawning hoki, with little bycatch. The other two tows on less dense marks in Pegasus Canyon caught much less hoki, with bycatch of red cod and black sharks.

A total of 1975 fish of 24 different species were measured during this survey. Otoliths and detailed biological data (including individual fish weights and gonad weights) were collected from 237 hoki. Genetic samples (fin clips in 99% ethanol) were collected from 100 hoki from Cook Strait and 100 hoki from Pegasus Canyon and were stored at NIWA.

3.2.3 Camera data

Four attempts were made to collect photographs showing the tilt angle of spawning hoki *in situ*. These were only partially successful. Hoki seem to have actively avoided the camera system. In addition, to position the camera within the hoki mark, it was necessary to find a very high density of fish close to the seabed and this could only be achieved once (station 14), in Cook Strait Canyon during the period when fishing vessels were excluded by the 1–7 August spawning closure. About 50 suitable photographs were collected (e.g., Figure 8). Tilt angles will be estimated and compared with previous data (Dunford et al. 2015).

3.2.4 CTD data

Fifteen CTD profiles were obtained in conjunction with midwater trawls (12 in Cook Strait, including the gear trial, and 3 in Pegasus Canyon). The average water temperature in Cook Strait over the entire depth range was 12.1 ºC, with an average salinity of 34.8 PSU. Estimates of sound absorption from individual CTD profiles in 2019 ranged from 8.79 to 9.10 dB km^{-1}, with an average of 8.96 dB km^{-1}. This was similar to the average sound absorption estimated in Cook Strait in 2015 (8.93 dB km^{-1}, O'Driscoll et al. 2016; no CTD profiles were obtained from Cook Strait during the 2017 survey). The three profiles in Pegasus Canyon showed an average temperature of 9.6 ºC, an average salinity of 34.5 PSU, and a calculated sound absorption of 9.20 dB km^{-1}, which was also similar to that estimated for this area in 2006 (9.20 dB km^{-1}, O'Driscoll 2007) and 2008 (9.22 dB km^{-1}, O'Driscoll 2009).

3.3 Mark identification

3.3.1 Acoustic mark types

Marks were similar to those observed in previous surveys from 2001–17. Example echograms of some of these mark types are shown in Figures 9–13. Further examples are provided by O'Driscoll (2002b, 2003, 2007, 2009, 2012), O'Driscoll & Dunford (2008), O'Driscoll & Macaulay (2009, 2010), O'Driscoll et al. (2015, 2016), and O'Driscoll & Escobar-Flores (2018).

1. Hoki schools ("hok")
Hoki school marks are characterised by relatively high acoustic return, with clearly defined edges, typically occurring at 200–500 m water depth, and often in midwater over canyon features. The densest hoki school

marks were observed in Cook Strait Canyon, but schools were also observed in Nicholson Canyon (e.g., Figure 9) and in Pegasus Canyon (e.g., Figure 10).

2. Hoki bottom fuzz (“bmix”)
Hoki bottom fuzz marks are diffuse, low-density layers adjoining the seabed and extending more than 50 m above it. These are usually in water depths shallower than 300 m. This mark type was commonly observed in the Narrows Basin (e.g., Figure 11) and over the Terawhiti Sill.

3. Hoki pelagic fuzz (“pmix”)
Hoki pelagic fuzz marks are characterised by low acoustic return, relatively constant depth within the 200–600 m range, typically over deep waters (500–1000 m), and often showing single target echoes within the layers. In 2019, these marks were common in outer Cook Strait Canyon (e.g., Figure 12), in the deep water between Cook and Wairarapa Canyons, in outer Pegasus Canyon, and in Conway Trough (e.g., Figure 13), and associated with hoki school marks in Cook Strait and Nicholson Canyons.

4. Bottom non-hoki (“b”)
Bottom non-hoki marks are bottom-referenced layers or schools, which were typically denser and shallower (less than 200 m depth) than hoki bottom fuzz layers. Bottom non-hoki marks were observed on one transect in 2019 in Nicholson Canyon. Previous research trawling on this mark type had catches dominated by ling, however the mark seen in 2019 may have been bluenose or redbait.

5. Jack mackerel (“jma”)
Jack mackerel marks are strong surface-referenced layers consisting of small schools and strong single targets at depths of 50 to 200 m. As in previous surveys, jack mackerel marks were usually observed in the Narrows Basin (e.g., Figure 11), but were also observed in Nicholson Canyon, Terawhiti Sill, and in the deep water between Cook and Wairarapa Canyons.

6. Mesopelagic layers (‘p”)
Mesopelagic layers are strong surface-referenced marks usually occurring between 0 and 300 m depth and exhibiting strong diurnal vertical migration patterns. Mesopelagic layers were widespread throughout the survey areas (e.g., Figures 12–13). Targeted trawling on this mark type in the past only caught a few very small (less than 30 cm) hoki.

7. Spiny dogfish (“spd”)
Spiny dogfish marks are characteristically surface-referenced marks, similar to jack mackerel marks, and consisted of small schools and single targets at depths of 100–200 m, usually above hoki schools marks. Midwater spiny dogfish marks were sometimes observed in Cook Strait Canyon during the 2019 survey. Livingston (1990) found that midwater aggregations of spiny dogfish above hoki schools were feeding on recently spawned hoki eggs.

3.3.2 Mark identification trawls

Mark identification trawls were carried out on four of the seven mark types (Table 5). No trawls were targeted at mesopelagic, spiny dogfish, or bottom non-hoki marks in 2019. Tows targeted on these mark types in previous years have typically caught less than 10% hoki.

Two trawls on hoki schools in Nicholson Canyon and Pegasus Canyon caught 97% and 99% of hoki by weight, respectively (Table 5). Four tows targeted at hoki pelagic fuzz marks in Cook Strait caught mostly hoki (50–98% hoki), but catches were much lower than from hoki schools (Table 5). Two trawls on pelagic fuzz in Pegasus Canyon caught 17% and 38% hoki respectively, with bycatch of red cod and black sharks (*Dalatias licha*). Three trawls on bottom fuzz marks in the Narrows Basin caught between 34% and 83% hoki (Table 5). Tows on jack mackerel marks in the Narrows Basin, Terawhiti Sill, and in the deepwater between Cook Strait and Wairarapa Canyons caught predominantly jack mackerel and less than 5% hoki (Table 5).

The proportions of hoki in trawls targeted at hoki schools, hoki pelagic fuzz, and hoki bottom fuzz marks in Cook Strait during 2019 were within the ranges caught from these mark types observed in previous surveys (Figure 14). The results suggest that there was a lower proportion of hoki in hoki fuzz marks in Pegasus Canyon compared with Cook Strait. This was also the case in 2006 (O'Driscoll 2007) and 2008 (O'Driscoll 2009). However, the number of tows on ECSI hoki fuzz marks in all three surveys were very small (only 2–3 tows). Further trawling on hoki fuzz mark types with a variety of gears is required in future surveys to help improve estimates of species composition on the ECSI spawning grounds.

3.3.3 Processing of acoustic backscatter data

Acoustic backscatter from regions corresponding to hoki schools, hoki bottom fuzz, and hoki pelagic fuzz were integrated to obtain acoustic density estimates, even though it is known that hoki fuzz marks also contain a proportion of other species (Figure 14). This is consistent with data analysis practice in previous years (O'Driscoll 2002a). No species decomposition of acoustic backscatter in mixed layers was attempted because of the low number of trawls and uncertainty associated with the relative catchability of different species in the midwater trawl. If there was a change in the proportion of hoki in fuzz marks over time (as suggested by O'Driscoll (2006) for bottom fuzz marks) this approach will lead to bias in the relative abundance estimates. However, the Monte Carlo estimation of survey uncertainty will incorporate some of this potential bias because the lognormal distribution of uncertainty associated with species mix is very broad (see Table 2). The observed species mix from trawls in 2019 was within the bounds of this lognormal distribution. In section 3.6, abundance estimates are presented for hoki school marks only (where mark identification is relatively certain), as well as for hoki school and hoki fuzz marks combined.

3.4 Distribution of hoki backscatter

3.4.1 Cook Strait

Expanding symbol plots show the spatial distribution of hoki backscatter along each transect during the seven snapshots of Cook Strait (Figure 15). As in previous years, hoki tended to be aggregated in two main regions within Cook Strait Canyon: in the shallower water at the head (northwestern end) of the canyon (as in snapshots 2–3 and 5 in 2019); and on the south side of the outer canyon close to the boundary between strata 2 and 5A (as in snapshot 1). In 2019, hoki distribution was intermediate in snapshots 4, 6, and 7, with hoki spread along the southern side of the middle part of the Cook Strait Canyon. High densities of hoki were also observed in Nicholson Canyon during snapshot 2.

Most of the acoustic backscatter in the deep water between Cook Strait and Wairarapa Canyons (stratum 5B) came from pelagic fuzz marks and densities were relatively low (Figure 15). Acoustic densities were also generally low in the Narrows Basin (stratum 1) and over the Terawhiti Sill (stratum 6), and most of the backscatter from these areas was from bottom fuzz marks.

3.4.2 East coast South Island

The strongest marks were associated with hoki schools in south Pegasus Canyon during the first snapshot (Figure 16), with densities comparable with those observed in Cook Strait Canyon (see Figure 10). Elsewhere, the densities of acoustic backscatter in the ECSI spawning areas in Pegasus Canyon (Figure 16) and Conway Trough (Figure 17) were generally weak. Pelagic fuzz marks were spread over a wide area in northern Pegasus Canyon (stratum PCA) and over the Conway Trough.

3.5 Hoki size and maturity

Although the number of research trawls in 2019 was low (14 tows) and sample sizes were small (Table 6), there was variation in hoki length frequency distributions between strata in Cook Strait (Figure 18) and between areas (Figure 19). Within Cook Strait, the largest hoki were caught in Nicholson Canyon (stratum 3, mean length of 64.1 cm), with the smallest in the outer Cook Strait Canyon (stratum 5A, mean = 38.6 cm) (Table 6). The overall mean length from research trawls in Cook Strait was 63.1 cm, which was much smaller than the average size of hoki in the Cook Strait commercial catch (76.5 cm, see Figure 5), which is because research trawls were carried out away from the main commercial fishing grounds in Cook Strait Canyon (stratum 2).

The hoki catch in inner Pegasus Canyon was dominated by males. Fewer hoki smaller than 60 cm were caught in Pegasus Canyon than in Cook Strait and the mean length was higher (66.9 cm) (Figure 19).

The length modes centred on about 45–55 cm and 60–65 cm for both males and females in Figure 19 correspond to hoki from the 2017 and 2016 year classes respectively, seen in 2019 at ages 2 and 3. There were also a few age 1 fish (28–35 cm) from the 2018 year class caught by research trawls.

A subsample of 306 hoki was weighed during the 2019 survey. The derived length-weight relationship ($R^2 = 0.99$) from these fish was:

$$w = (3.473 * 10^{-6})\, L^{2.9704} \qquad (3)$$

This relationship gave a weight about 2.6% higher for a hoki of 75 cm than that obtained using the generic relationship of Francis (2003), likely because almost all adult hoki caught during the survey were in spawning condition.

When *r* (the ratio used to convert hoki backscatter to biomass) was calculated from the hoki length frequencies from research tows using the length-weight relationship estimated from the survey (equation (3)) and the TS-length relationship of Dunford et al. (2015) (equation (2)), the ratio was 7790 kg m^{-2} for Cook Strait and 7762 kg m^{-2} for Pegasus Canyon.

The ratio for Cook Strait was lower than the value of *r* obtained from the commercial fishery in 2019 using the standard approach (section 3.1.1, $r = 8155$ kg m^{-2}) because of the smaller average size of hoki caught in research tows. Ideally, hoki TS values would be strata- and snapshot-specific, based on length frequencies from research trawls during the acoustic survey. In practice, this level of research fishing is not possible and *r* calculated from commercial tows (which provide extensive sampling of the main spawning marks) is used to estimate biomass. The length frequency of hoki caught in the commercial fishery may not represent the length frequency of the underlying spawning population due to gear selectivity, or targeting of fish of certain size, or at certain depth ranges. However, the variation in length in the commercial catch is likely to give a realistic idea of the level of interannual variability in fish size (O'Driscoll 2002a).

The ratio for Pegasus Canyon calculated from research tows was slightly higher than the value of *r* obtained from commercial data for the ECSI (section 3.1.2, $r = 7575$ kg m^{-2}). Because of the much greater number of commercial tows sampled (36 observer samples from the ECSI in 2019), the ratio of *r* calculated from commercial data was used when estimating hoki biomass on the ECSI. Although many of the observed tows were outside the main acoustic survey strata and after the ECSI survey finished (21 August to 24 September), commercial tows caught spawning hoki (see section 3.1.2) and were probably representative of size composition in the area.

The gonad stages of hoki caught in research trawls are given in Table 7. Almost all hoki sampled during the acoustic survey were in spawning condition (stages 3–7), both in Cook Strait (96%) and in Pegasus Canyon (89%). Most males were ripe or running ripe (stages 4 and 5), and most females were maturing, ripe, or partially spent (stages 3, 4, and 6). There were no clear indications of spawning events in gonad stage data from research trawls. The number of tows carried out during each snapshot was small, and temporal patterns were confounded by the spatial distribution of tows.

3.6 Hoki abundance estimates

3.6.1 Cook Strait

Hoki abundance estimates by snapshot and strata are given in Table 8 and plotted in Figure 20. Hoki abundance in Cook Strait was highest in snapshot 1 (18–19 July) and snapshot 3 (29–30 July) at 124 000 t, with the lowest estimate of 46 000 t in snapshot 7 on 18–19 August. Differences between individual snapshots are probably due to sampling variability (transect location and fish behaviour) as well as changes in abundance. High variability in abundance between snapshots was also observed in previous surveys (e.g., in 2002, 2006, 2007, 2011, 2013, and 2015 in Figure 21). Sampling precision (CV) of individual snapshots ranged between 14% and 27% (Table 8).

When results from Table 8 were averaged over all snapshots, 61% of the hoki biomass was in stratum 2, 14% in stratum 1, 9% in stratum 5B, 7% in stratum 5A, 5% in stratum 3, and 3% in stratum 6. Hoki densities in strata 1 and 5B were generally low (see Figure 15), and the importance of these strata to the overall biomass was due to their relatively large areas. The contribution of biomass from outside Cook Strait Canyon (stratum 2) may also be overestimated because most of the estimated biomass in the other strata was from hoki fuzz marks which contain other species (Table 9).

The average proportion of the biomass from hoki schools in 2019 was 53% (Table 9). This was similar to the proportion in school marks in 2017 (54%), and within the range of proportions in previous surveys (30–78% of hoki in schools in 1991–2015). Most (82%) of the hoki observed in stratum 2 in 2019 were in schools (Table 9). Hoki schools were also observed in strata 3 and 5A. As in previous surveys, changes in abundance over the survey period were driven mainly by changes in the biomass of hoki schools (see Figure 20). The biomass from hoki fuzz marks remained relatively constant between 27 000 t and 57 000 t throughout the survey period.

The mean abundance from snapshots 1–7 was 91 000 t (see Table 8). The average of the snapshot coefficients of variation was 8%. The variance of the abundance estimates from the six snapshots was 12%. The similarity of the two estimates of sampling variance provides evidence that variation in estimated biomass between individual snapshots was consistent with sampling variability.

The overall survey weighting estimated from the Monte Carlo simulation model for Cook Strait was 36% (Table 10). As in previous Cook Strait surveys (O’Driscoll 2004), timing (including uncertainties about plateau timing and residence time), sampling error, and mark identification were the major sources of uncertainty (Table 10). Uncertainties due to calibration, detectability, and TS contributed relatively little to the overall CV. However, incorrect choice of TS and calibration coefficients have the potential to introduce bias in estimates, which is not reflected in the CV in Table 10.

The abundance index for 2019 was similar to (11% lower than) the estimate from the previous survey in 2017 (102 000 t), less than half of the estimate in 2015 (204 000 t), and the lowest estimate since 2008 (Table 11).

3.6.2 East coast South Island

The two snapshots of Pegasus Canyon gave abundance estimates of 60 000 t and 51 000 t respectively (Table 12). Although the snapshots were less than a day apart, there was some redistribution of fish between strata, with more hoki in the southern canyon (stratum PCB) during the first snapshot (see Figure 16). The abundance estimate from the single snapshot of Conway Trough was 15 000 t (Table 12).

On average, 64% of the hoki biomass in Pegasus Canyon came from hoki schools, with a much higher proportion of schooling hoki in stratum PCB (Table 13). The overall proportion of hoki in schools was in the range of previous surveys in 2002–13, when between 33% and 78% of the biomass in Pegasus Canyon came from schools (Table 14). None of the hoki in Conway Trough were in schools in 2019. In previous surveys of Conway Trough in 2002–08, 8–27% of hoki were in schools (Table 14).

The average abundance index of 55 000 t from Pegasus Canyon in 2019 was similar to that from the previous estimate based on one snapshot on 20 August 2013 (64 000 t), and from the average of 7 snapshots from 3–11 September 2002 (60 000 t), and higher than estimates from 2003–08 (Tables 14–15). However, it is difficult to interpret the apparent changes in abundance on the ECSI because of the different timing of the six surveys (see Table 14). Because the estimated abundance in Cook Strait has declined (see Table 11), the relative contribution of Pegasus Canyon was highest in 2019 (Table 15).

The abundance estimate of 15 000 t from Conway Trough was within the range of estimates from previous surveys in 2002–2008 (14 000–26 000 t) (Tables 14 and 16). All these biomass values for Conway Trough likely overestimate hoki abundance because 73% (in 2002) to 100% (in 2019) of the hoki were in pelagic fuzz marks which contain other species. In 2008, a single trawl on this mark type caught only 41% hoki by weight (O'Driscoll 2009). No trawls were carried out in Conway Trough during surveys in 2002, 2003, 2006, or 2019.

4. DISCUSSION

Seven acoustic snapshots of the hoki spawning abundance in Cook Strait were completed from *Kaharoa* during winter 2019. This was the first Cook Strait survey using *Kaharoa* since 2008 (surveys in 2009–15 were carried out from commercial fishing vessels, and the 2017 survey was from the coastal research vessel *Ikatere*). The use of *Kaharoa* as a dedicated vessel allowed greater control over the timing of snapshots, increased mark identification trawling, and made it possible to collect experimental data.

Weather during the 2019 survey period was good enough to allow collection of high-quality acoustic data using the vessel echosounder with hull-mounted transducers. However, if future Cook Strait surveys are to be from *Kaharoa*, the use of towed acoustic systems, which increase the range of weather conditions suitable for data collection, should be investigated. Towed systems were used previously from *Kaharoa* (e.g., O'Driscoll 2009), but it was not possible to use the towed system for the 2019 voyage because the decision to use *Kaharoa* as the survey vessel was made too late to allow the associated winches and deployment/retrieval systems to be overhauled and fitted.

The acoustic abundance index from Cook Strait in 2019 was 11% lower than the equivalent index from the 2017 survey, and the lowest since 2008 (see Table 11). The survey weighting, which includes uncertainty associated with survey timing, sampling precision, mark identification, acoustic detectability, calibration, and target strength, was 36% (see Table 10). This CV was within the range of estimated uncertainty in research and industry vessel surveys since 2001 (CV 30–46% in Table 11), reflecting the consistent survey design and execution over this period.

The 2019 survey also covered other eastern spawning grounds, with two snapshots of Pegasus Canyon and one of Conway Trough. The combined acoustic abundance estimate for Pegasus Canyon and Conway Trough of 70 000 t was 76% of the estimate from Cook Strait (91 000 t). However, the comparison of relative acoustic abundance indices from the two areas should be made with caution because the interpretation of acoustic abundance indices (based on the average of multiple snapshots) depend on assumptions about the spawning season, plateau interval, and residence time (Cordue et al. 1992, Coombs & Cordue 1995), which may be different between the ECSI and Cook Strait.

The 6-week duration of the survey allowed good coverage in Cook Strait, while still allowing time to survey the ECSI spawning areas and carry out limited experimental work. However, given the apparent importance of the ECSI spawning grounds (even with the caveats above), future surveys should include more effort off the ECSI. Anecdotal evidence from fishers and the timing of the commercial catch suggests that peak biomass off the ECSI is probably in late August and early September (see Figure 3).

5. MANAGEMENT IMPLICATIONS

The halving in hoki abundance estimates from Cook Strait between 2015 and 2017 was not consistent with predictions from the 2019 hoki stock assessment, which suggests that the spawning biomass of the eastern hoki stock is increasing or stable and above target levels (Fisheries New Zealand 2019). The acoustic estimate from 2019 was similar to that in 2017, which was lower than all surveys since 2009, supporting the theory of a recent decline in the eastern spawning population. This is also in agreement with the observation that abundance of larger (age 3+ and older) hoki declined by 26% in the Chatham Rise trawl survey core area from 2016 to 2018 (Stevens et al. 2018).

Like previous years, the 2019 survey confirmed the presence of significant hoki spawning aggregations off the ECSI, particularly in Pegasus Canyon. Although comparisons of relative levels of biomass are difficult due to differences in survey timing and a limited number of snapshots on the ECSI, this suggests that abundance on the ECSI has remained more stable since 2013 than in Cook Strait.

6. ACKNOWLEDGMENTS

Thanks to Lindsay Copland and Evan Solly (skippers) and the crew of *Kaharo*a whose experience and skills ensured a successful voyage. Dan MacGibbon, Nick Eton, Alexandre Schimel, Ben Lennard, and Yoann Ladroit from NIWA participated in the voyage and assisted with data collection. This report was reviewed by Alexandre Schimel (NIWA). Due to the nature of this voyage, with short trips from Wellington, we were able to share the *Kaharoa* experience with Sonja Hempel and Gretchen Skea (Fisheries New Zealand), Kate Evans and Richie Robinson (New Zealand Geographic magazine), and Bex Parsons-King and Stu Mackay (NIWA communications team). We thank them for their participation and providing the resulting science outreach.

7. REFERENCES

Coombs, R.F.; Cordue, P.L. (1995). Evolution of a stock assessment tool: acoustic surveys of spawning hoki (*Macruronus novaezelandiae*) off the west coast of South Island, New Zealand, 1985–91. *New Zealand Journal of Marine and Freshwater Research 29*: 175–194.

Cordue, P.L.; Ballara, S.L. (2001). An acoustic survey of spawning hoki in Cook Strait during winter 1999. *New Zealand Fisheries Assessment Report 2001/15.* 18 p.

Cordue, P.L.; McAllister, M.K.; Pikitch, E.K.; Sullivan, K.J. (1992). Stock assessment of hoki 1991. New Zealand Fisheries Assessment Research Document 92/10. 41 p. (Unpublished report held by NIWA library, Wellington.)

Demer, D.A.; Berger, L.; Bernasconi, M.; Bethke, E.; Boswell, K.; Chu, D.; Domokos, R.; et al. (2015). Calibration of acoustic instruments. *ICES Cooperative Research Report No. 326*. 133 p.

Doonan, I.J.; Coombs, R.F.; McClatchie, S. (2003). The absorption of sound in seawater in relation to the estimation of deep-water fish biomass. *ICES Journal of Marine Science 60*: 1047–1055.

Dunford, A.J.; O'Driscoll, R.L.; Oeffner, J. (2015). Improvements in estimating an acoustic target strength-length relationship for hoki (*Macruronus novaezelandiae*). *Fisheries Research 162:*12–19.

Fisheries New Zealand (2019). Fisheries Assessment Plenary, May 2019: stock assessments and stock status. Compiled by the Fisheries Science and Information Group, Fisheries New Zealand, Wellington, New Zealand. 1641 p.

Fofonoff, P.; Millard, R., Jr (1983). Algorithms for computation of fundamental properties of seawater. *UNESCO Technical Papers in Marine Science 44*. 53 p.

Francis, R.I.C.C. (2003). Analyses supporting the 2002 stock assessment of hoki. *New Zealand Fisheries Assessment Report 2003/5.* 34 p.

Jolly, G.M.; Hampton, I. (1990). A stratified random transect design for acoustic surveys of fish stocks. *Canadian Journal of Fisheries and Aquatic Sciences 47*: 1282–1291.

Ladroit, Y. (2017). ESP3: an open-source software for fisheries acoustic data processing. https://bitbucket.org/echoanalysis/esp3
Livingston, M.E. (1990). Spawning hoki (*Macruronus novaezelandae* Hector) concentrations in Cook Strait and off the east coast of the South Island, New Zealand, August–September 1987. *New Zealand Journal of Marine and Freshwater Research 24*: 503–517.
MacLennan, D.N.; Fernandes P.G.; Dalen J. (2002). A consistent approach to definitions and symbols in fisheries acoustics. *ICES Journal of Marine Science 59*: 365–369.
McKenzie, A. (2018). Assessment of hoki (*Macruronus novaezelandiae*) in 2017. *New Zealand Fisheries Assessment Report 2018/40.* 101 p.
O'Driscoll, R.L. (2002a). Review of acoustic data inputs for the 2002 hoki stock assessment. *New Zealand Fisheries Assessment Report 2002/36*. 64 p.
O'Driscoll, R.L. (2002b). Acoustic survey of spawning hoki in Cook Strait during winter 2001. *New Zealand Fisheries Assessment Report 2002/37*. 35 p.
O'Driscoll, R.L. (2003). Acoustic survey of spawning hoki in Cook Strait during winter 2002. *New Zealand Fisheries Assessment Report 2003/27*. 34 p.
O'Driscoll, R.L. (2004). Estimating uncertainty associated with acoustic surveys of spawning hoki (*Macruronus novaezelandiae*) in Cook Strait, New Zealand. *ICES Journal of Marine Science 61*: 84–97.
O'Driscoll, R.L. (2006). Acoustic survey of spawning hoki in Cook Strait during winter 2005, and revision of hoki acoustic abundance indices for Cook Strait and the west coast South Island. *New Zealand Fisheries Assessment Report 2006/44*. 46 p.
O'Driscoll, R.L. (2007). Acoustic survey of spawning hoki in Cook Strait and off the east coast South Island during winter 2006. *New Zealand Fisheries Assessment Report 2007/21*. 52 p.
O'Driscoll, R.L. (2009). Acoustic survey of spawning hoki in Cook Strait and off the east coast South Island during winter 2008. *New Zealand Fisheries Assessment Report 2009/17*. 52 p.
O'Driscoll, R.L. (2012). Acoustic survey of spawning hoki in Cook Strait during winter 2011. *New Zealand Fisheries Assessment Report 2012/17*. 50 p.
O'Driscoll, R.L.; Bagley, N.W.; Macaulay, G.J.; Dunford, A.J. (2004). Acoustic surveys of spawning hoki off South Island on FV *Independent 1* in winter 2003. *New Zealand Fisheries Assessment Report 2004/29*. 48 p.
O'Driscoll, R.L.; Dunford, A.J. (2008). Acoustic survey of spawning hoki in Cook Strait during winter 2007. NIWA Client Report WLG2008-1 for The Deepwater Group Ltd. 44 p.
O'Driscoll, R.L.; Escobar-Flores, P. (2018). Acoustic survey of spawning hoki in Cook Strait during winter 2017. *New Zealand Fisheries Assessment Report 2018/12*. 39 p.
O'Driscoll, R.L.; Ladroit, Y.; Dunford, A.J.: MacGibbon, D.J. (2015). Acoustic survey of spawning hoki in Cook Strait and Pegasus Canyon during winter 2013. *New Zealand Fisheries Assessment Report 2015/04*. 51 p.
O'Driscoll, R.L.; Ladroit, Y.; Dunford, A.J.: MacGibbon, D.J. (2016). Acoustic survey of spawning hoki in Cook Strait during winter 2015 and update of acoustic q priors for hoki stock assessment modelling. *New Zealand Fisheries Assessment Report 2016/44*. 55 p.
O'Driscoll, R.L.; Macaulay, G.J. (2009). Industry acoustic survey of spawning hoki in Cook Strait during winter 2008. NIWA Client Report WLG2009-8 for The Deepwater Group Ltd. 40 p.
O'Driscoll, R.L.; Macaulay, G.J. (2010). Industry acoustic survey of spawning hoki in Cook Strait during winter 2009. NIWA Client Report WLG2010-13 for The Deepwater Group Ltd. 56 p.
Rose, G.; Gauthier, S.; Lawson, G. (2000). Acoustic surveys in the full monte: simulating uncertainty. *Aquatic Living Resources 13*: 367–372.
Simmonds, E.J.; MacLennan, D.N. (2005). Fisheries acoustics. Second edition. Blackwell Science, Oxford. 437 p.
Stevens, D.W.; O'Driscoll, R.L.; Ballara, S.L.; Schimel, A.C.G. (2018). Trawl survey of hoki and middle depth species on the Chatham Rise, January 2018 (TAN1801). *New Zealand Fisheries Assessment Report 2018/41.* 111 p.

8. TABLES

Table 1: Stratum boundaries, areas and transect allocation in the 2019 acoustic survey of spawning hoki in Cook Strait and off the east coast South Island (ECSI). Stratum locations are shown in Figures 1 and 2.

Area	Stratum	Name	Boundary	Area (km^2)	No. of transects
Cook Strait	1	Narrows Basin	200–200 m	330	4
	2	Cook Strait Canyon	180–180 m	220	9
	3	Nicholson Canyon	200–200 m	55	4
	5A	Cook Strait Canyon extension	position to 200 m	90	3
	5B	Deep water	position to 200 m	215	3
	6	Terawhiti Sill	200–200 m	65	4
ECSI	CT	Conway Trough	200–200 m	171	6
	PCA	North Pegasus Canyon	position to 200 m	270	6
	PCB	South Pegasus Canyon	200–200 m	63	4

Table 2: Values of parameters and their distributions used in Monte Carlo uncertainty simulations to determine model weighting (from O'Driscoll 2004).

Term	Notation	Distribution	Values*
Mean arrival date	$\bar{d}$	Uniform	1 July–9 August
Mean residence time	$\bar{r}$	Uniform	24–47 days
Individual arrival date	d_i	Normal	$\bar{d}$ (5 days)
Individual residence time	r_i	Normal	$\bar{r}$ (10 days)
Sampling	s	Normal	1.0 (snapshot CV)
Detectability	D	Uniform	0.85–0.97
Mark identification – 'fuzz' marks	Id_{fuzz}	Lognormal	0.78 (0.72)
Mark identification – 'school' marks	Id_{school}	Lognormal	0.10 (0.16)
Calibration	cal	Uniform	cal ± 0.2 dB
Target strength§	TS	Uniform	TS ± 0.5 dB

* For uniform distribution, values are ranges; for normal distributions, values are means with standard deviations (in parentheses); for lognormal distributions, values are the mean and standard deviation (in parentheses) of $\log_e$(variable).

§ Uncertainty associated with TS arose from variation in fish size, and from differences in the slope of alternative TS-length relationships. Potential bias due to differences in the intercept of alternative TS-length models was ignored because it will not affect the relative values of acoustic indices (see O'Driscoll 2004 for details).

Table 3: Summary of snapshots carried out during 2019 Cook Strait hoki acoustic survey. Times are NZST.

Snapshot	Start time	End time	No. of transects	No. of trawls	No. of camera drops
1	18 Jul 16:51	19 Jul 23:14	28	1*	0
2	22 Jul 10:39	23 Jul 13:17	28	3	0
3	23 Jul 18:23	25 Jul 22:05	28	5	2
4	29 Jul 12:22	30 Jul 10:51	28	0	0
5	5 Aug 12:50	6 Aug 22:30	28	2	2
6	12 Aug 09:47	13 Aug 10:02	28	1	0
7	18 Aug 17:48	19 Aug 16:25	28	0	0

* Trawl in snapshot 1 was a gear trial with codend open

Table 4: Summary of snapshots carried out during the acoustic survey of Pegasus Canyon and Conway Trough. Times are NZST.

Area	Snapshot	Start time	End time	No. of transects	No. of trawls
Pegasus Canyon	1	15 Aug 22:16	16 Aug 05:41	10	1
Pegasus Canyon	2	16 Aug 09:38	16 Aug 21:06	10	2
Conway Trough	1	17 Aug 02:35	17 Aug 07:18	6	0

Table 5: Summary and catch information from trawl stations carried out during 2019 hoki acoustic survey. Mark type refers to the categories described in section 3.3.1.: hoki school ("HOK"); hoki pelagic fuzz ("PMIX"); hoki bottom fuzz ("BMIX"); jack mackerel ("JMA"). Note that tow 1 was a gear trial with codend open. Stations 5, 6, 14, and 15 were camera drops.

				Catch (kg)						
Station	Snapshot	Stratum	Mark type	Hoki	Jack mackerel	Spiny dogfish	Ling	Rattails	Other	% Hoki
2	2	3	HOK	681	0	15	9	0	1	97
3	2	1	JMA	0	200	0	0	0	0	0
4	2	1	BMIX	265	61	8	17	0	42	67
7	3	5B	JMA	2	123	2	0	0	5	2
8	3	5B	PMIX	21	0	0	0	1	3	84
9	3	5A	PMIX	6	0	0	0	4	1	50
10	3	1	BMIX	33	0	2	0	0	63	34
11	3	6	JMA	9	241	0	0	0	3	4
12	5	1	BMIX	96	2	14	0	0	5	83
13	5	5B	PMIX	72	0	3	0	0	2	93
16	6	3	PMIX	152	0	1	0	0	2	98
17	1	PCB	HOK	2 200	0	7	0	0	7	99
18	2	PCA	PMIX	9	0	0	0	0	15	38
19	2	PCA	PMIX	20	0	0	0	2	93	17

Table 6: Mean length of hoki caught during the 2019 acoustic survey by stratum. Length frequency distributions are shown in Figures 18 and 19.

Stratum	No. trawls	No. hoki measured	Mean length (cm)	% female hoki
1	4	359	63.7	54.9
3	2	325	64.1	46.8
5A	1	21	38.6	42.9
5B	3	98	58.8	55.1
6	1	10	58.1	70.0
All Cook Strait	11	813	63.1	51.5
Pegasus Canyon	3	200	66.9	29.0

Table 7: Gonad stages of hoki caught in research trawls during the 2019 acoustic survey. Data are arranged by area and snapshot. Gonad stages are defined in Appendix 2.

		Cook Strait				Pegasus
Snapshot		2	3	5	6	1&2
Date		22 Jul	24 Jul	5Aug	12 Aug	16 Aug
Sex	Stage					
Male	1	0	7	3	0	8
	2	0	0	0	0	3
	3	10	6	10	2	15
	4	177	30	13	1	37
	5	64	29	13	1	70
	6	9	12	5	0	2
	7	1	0	1	0	2
Female	1	0	15	4	0	9
	2	0	0	0	0	1
	3	92	11	60	37	18
	4	38	3	17	10	17
	5	0	0	3	2	5
	6	47	4	11	14	6
	7	16	6	17	11	2

Table 8: Hoki acoustic abundance estimates from the 2019 Cook Strait survey by snapshot and stratum.

	Stratum biomass (‘000 t)						Total	Snapshot
Snapshot	1	2	3	5A	5B	6	(‘000 t)	CV
1	14	88	3	7	7	4	124	16
2	14	41	14	10	9	3	90	27
3	15	39	3	3	2	2	64	23
4	10	89	5	7	11	3	124	23
5	17	53	3	7	13	4	97	25
6	11	55	4	7	13	3	93	17
7	10	25	3	3	5	1	46	14
mean	13	56	5	6	9	3	91	8

Table 9: Percentage of the hoki abundance estimate from hoki school marks in each snapshot and strata for Cook Strait. Percentages were calculated in relation to abundance estimates in Table 8.

	Biomass in schools (%)						
Snapshot	1	2	3	5A	5B	6	Total
1	0	87	0	35	0	0	64
2	0	78	84	7	0	0	50
3	0	79	8	35	0	0	50
4	0	86	68	38	0	0	67
5	0	81	17	0	0	0	45
6	0	85	8	58	0	0	55
7	0	76	0	0	0	0	41
mean	0	82	27	25	0	0	53

Table 10: Results of Monte Carlo simulations to determine model weighting for the 2019 Cook Strait acoustic survey (see O'Driscoll 2004 for details). The CV for the survey is given in a stepwise cumulative fashion to allow the contribution of each component of the abundance estimation process to be assessed. 'Timing' refers to uncertainties associated with the timing of snapshots relative to the plateau height model and includes uncertainties associated with assumptions about fish arrival date and residence time.

Timing	0.279
+ Sampling	0.294
+ Detectability	0.294
+ Mark identification	0.342
+ Calibration	0.345
+ TS	0.357
Total	**0.36**

Table 11: Acoustic indices of hoki abundance for Cook Strait 1988–2019. All indices were re-calculated by O'Driscoll & Escobar-Flores (2018) using the acoustic TS derived from commercial length frequency data in each survey year using the most recent hoki TS-length relationship of Dunford et al. (2015). The 2019 estimate is the mean of snapshots 1–7.

Year	No. of accepted snapshots	Biomass ('000 t)	CV
1991	4	88	0.41
1993	4	283	0.52
1994	3	278	0.91
1995	4	194	0.61
1996	5	92	0.57
1997	6	141	0.40
1998	5	80	0.44
1999	6	114	0.36
2001	11	102	0.30
2002	9	145	0.35
2003	9	104	0.34
2005	9	59	0.32
2006	7	60	0.34
2007*	4	104	0.46
2008	7	82	0.30
2009*	5	166	0.39
2011*	6	141	0.35
2013*	7	168	0.30
2015*	5	204	0.33
2017	6	102	0.36
2019	7	91	0.36

* Surveys from industry vessels.

Table 12: Hoki acoustic abundance estimates from the 2019 east coast South Island survey by snapshot and stratum.

		Stratum biomass ('000 t)		Total	Snapshot
Area	Snapshot	PCA	PCB	('000 t)	CV
Pegasus Canyon	1	19	40	60	33
	2	35	16	51	25
	mean	27	28	55	21
		CT			
Conway Trough	1	15		15	8

Table 13: Percentage of the hoki abundance estimate from hoki school marks in each snapshot and strata for the east coast South Island. Percentages were calculated in relation to abundance estimates in Table 12.

		Biomass in schools (%)		
Area	Snapshot	PCA	PCB	Total
Pegasus Canyon	1	7	97	67
	2	41	100	60
	mean	24	98	64
		CT		
Conway Trough	1	0		0

Table 14: Hoki acoustic biomass estimates for previous ECSI hoki acoustic surveys by snapshot and stratum from 2002–13. Percentage of the biomass from hoki school marks is also given. These values have been revised from those in the original documents to use the most recent TS-length relationship for hoki (Dunford et al. 2015).

Year	Snapshot	Start date	End date	Biomass ('000 t)	Snapshot c.v.	% biomass in schools
2002	1	3 Sep	3 Sep	50	31	73
Pegasus Canyon	2	3 Sep	5 Sep	57	29	61
	3	5 Sep	6 Sep	47	21	88
	4	7 Sep	8 Sep	84	50	93
	5	8 Sep	9 Sep	54	40	87
	6	9 Sep	9 Sep	99	55	95
	7	10 Sep	11 Sep	26	15	46
	mean			60	19	78
Conway Trough	1	7 Sep	10 Sep	14	21	27
2003						
Pegasus Canyon	1	30 Jul	31 Jul	32	18	72
	2	18 Aug	18 Aug	61	31	71
	3	22 Aug	23 Aug	62	33	64
	4	11 Sep	12 Sep	26	12	26
	mean			45	16	58
Conway Trough	1	18 Aug	18 Aug	26	14	15
2006						
Pegasus Canyon	1	29 Jul	29 Jul	12	22	14
	2	23 Aug	23 Aug	19	41	56
	3	23 Aug	24 Aug	21	26	45
	mean			17	19	38
Conway Trough	1	30 Jul	30 Jul	24	12	8
2008						
Pegasus Canyon	1	14 Aug	15 Aug	20	9	25
	2	15 Aug	16 Aug	20	21	41
	mean			20	11	33
Conway Trough	1	14 Aug	14 Aug	20	32	14
	2	16 Aug	16 Aug	25	12	11
	mean			23	10	13
2013						
Pegasus Canyon	1	20 Aug	20 Aug	64	28	80

Table 15: Acoustic indices of hoki abundance for Pegasus Canyon 2002–19. All biomass values were estimated using the TS-length relationships of Dunford et al. (2015). % PC ref CS indicates the abundance in Pegasus Canyon as a percentage of the equivalent estimate from Cook Strait (see Table 11). Values for previous surveys by snapshot and stratum are given in Table 14.

Year	No. of snapshots	Biomass (‘000 t)	% PC ref CS
2002*	7	60	41
2003*	4	45	43
2006	3	17	28
2008	2	20	24
2013*	1	64	38
2019	2	55	60

* Surveys from industry vessels.

Table 16: Acoustic indices of hoki abundance for Conway Trough 2002–19. All biomass values were estimated using the TS-length relationships of Dunford et al. (2015). % Cook Strait indicates the abundance in Conway Trough as a percentage of the equivalent estimate from Cook Strait (see Table 11). Values for previous surveys by snapshot and stratum are given in Table 14.

Year	No. of snapshots	Biomass (‘000 t)	% Cook Strait
2002*	1	14	10
2003*	1	26	25
2006	1	24	40
2008	2	23	28
2019	1	15	16

* Surveys from industry vessels.

9. FIGURES

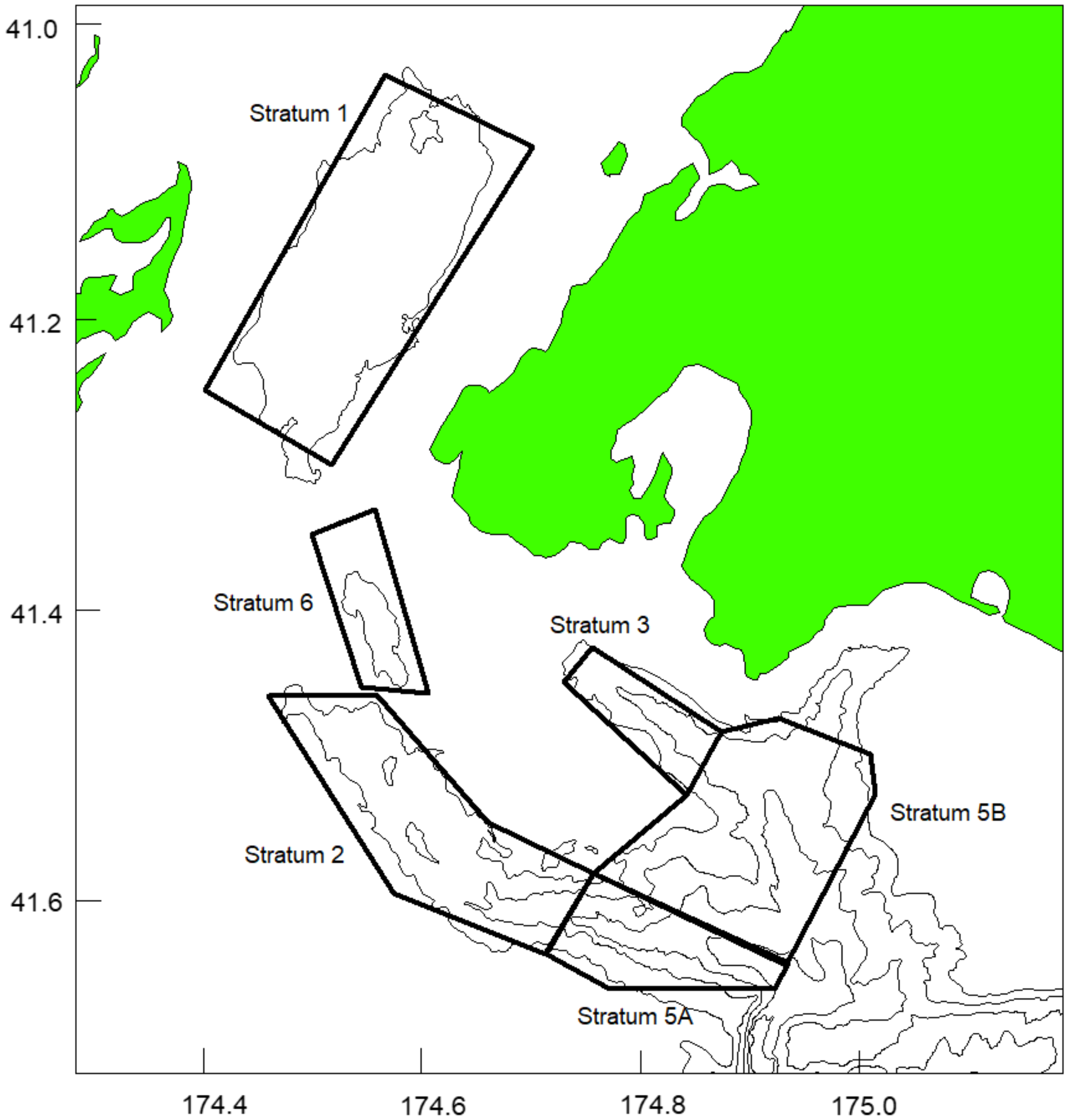

Figure 1: Stratum boundaries for the 2019 acoustic survey of Cook Strait spawning hoki: 1, Narrows Basin; 2, Cook Strait Canyon; 3, Nicholson Canyon; 5A, Cook Strait Canyon extension; 5B, Deepwater outside Nicholson and Wairarapa Canyons; 6, Terawhiti Sill. Depth contours are 250, 500, 750, and 1000 m.

Figure 2: Stratum boundaries for the east coast of South Island spawning grounds. The stratum names are: CT, Conway Trough; PCA, North Pegasus Canyon; PCB, South Pegasus Canyon. Depth contours are 500 and 1000 m.

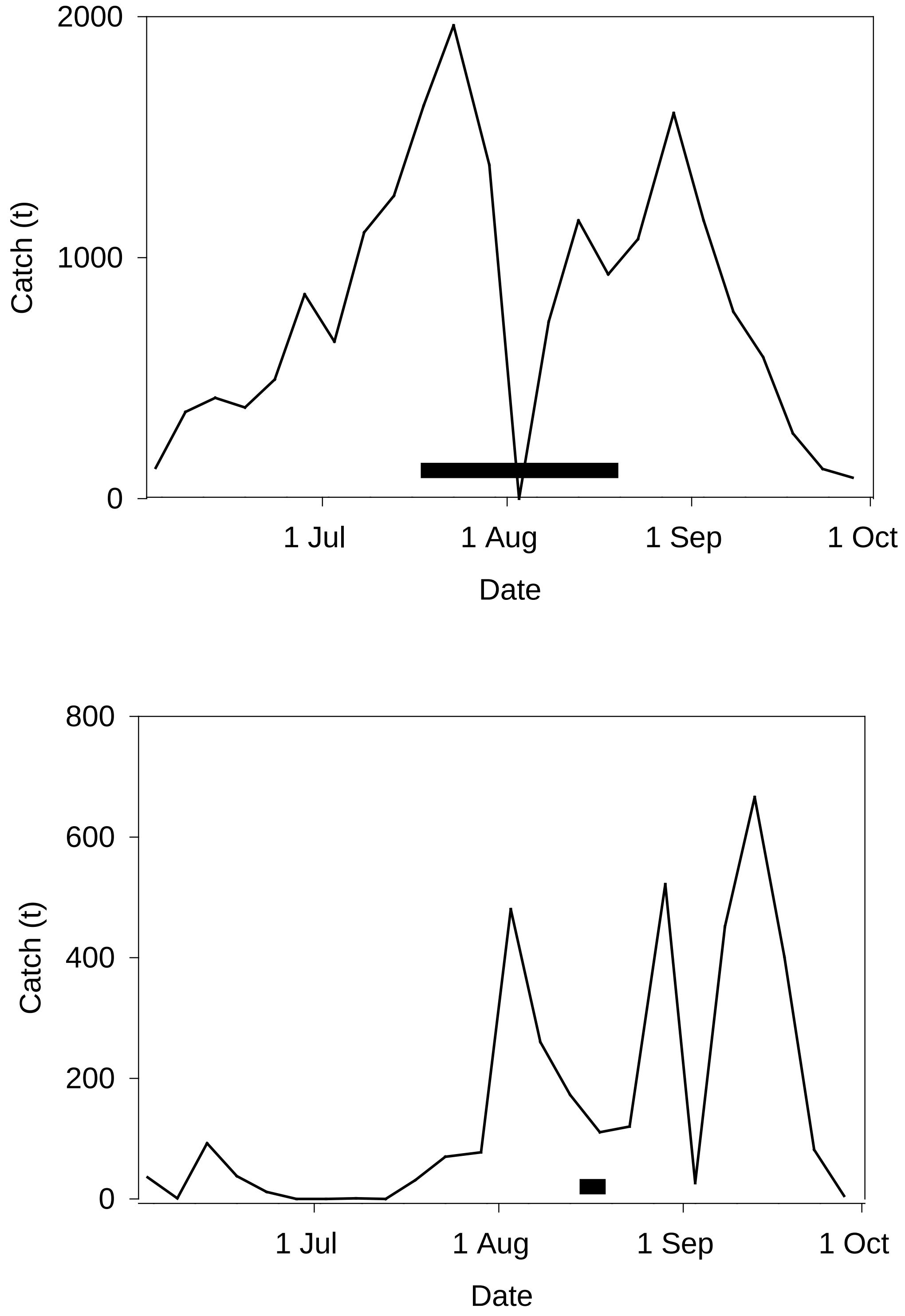

Figure 3: Timing of acoustic surveys in 2019 (bars in bold along the x axes) in relation to the commercial hoki catch from Cook Strait (upper panel) and ECSI (lower panel) in 5-day periods.

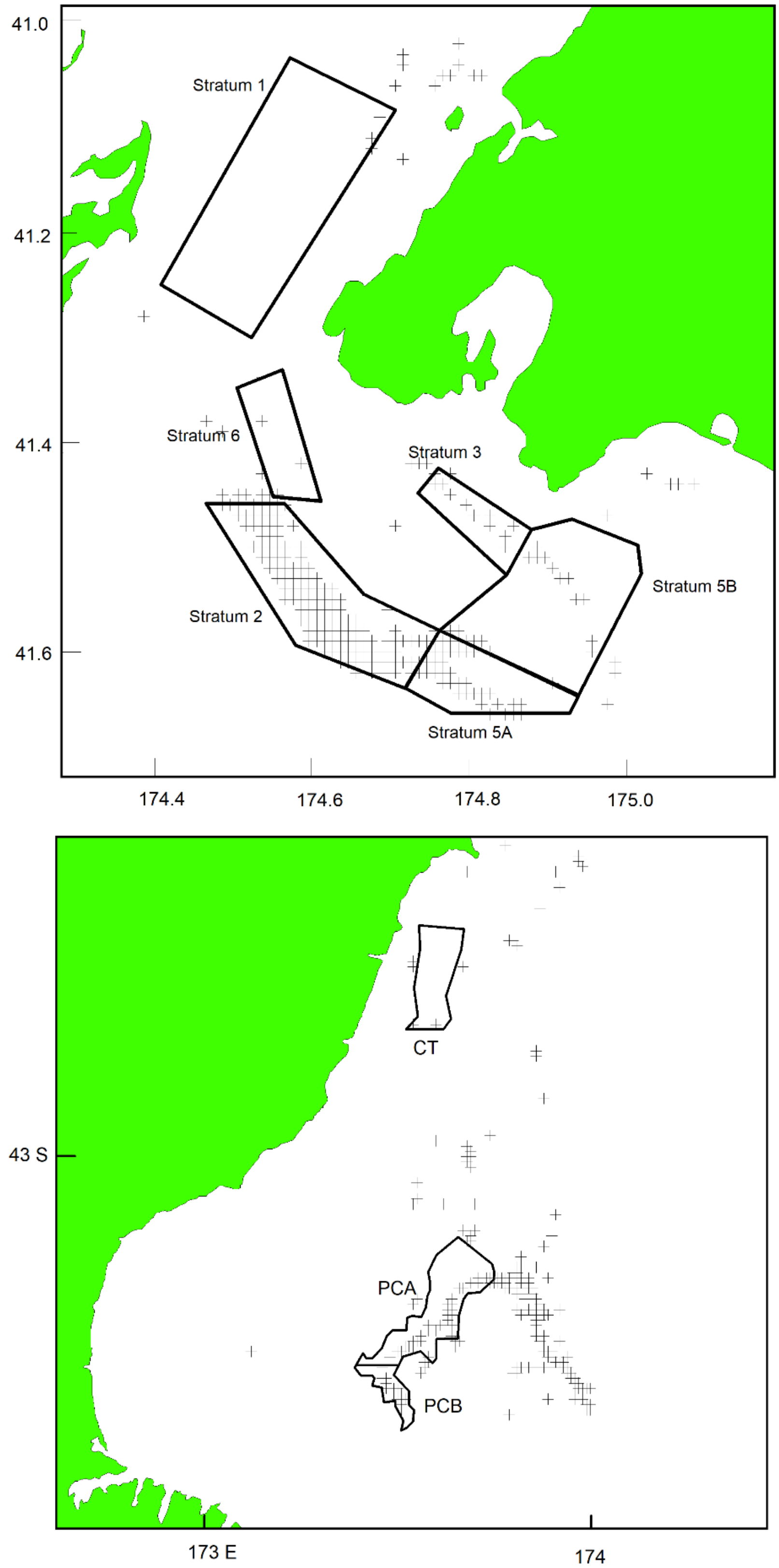

Figure 4: Distribution of recorded start positions of tows catching hoki (crosses) in Cook Strait (upper panel) and ECSI (lower panel) from 1 June to 30 September 2019 in relation to the acoustic survey boundaries. Note that data were not checked for positional errors and one cross can represent multiple tows.

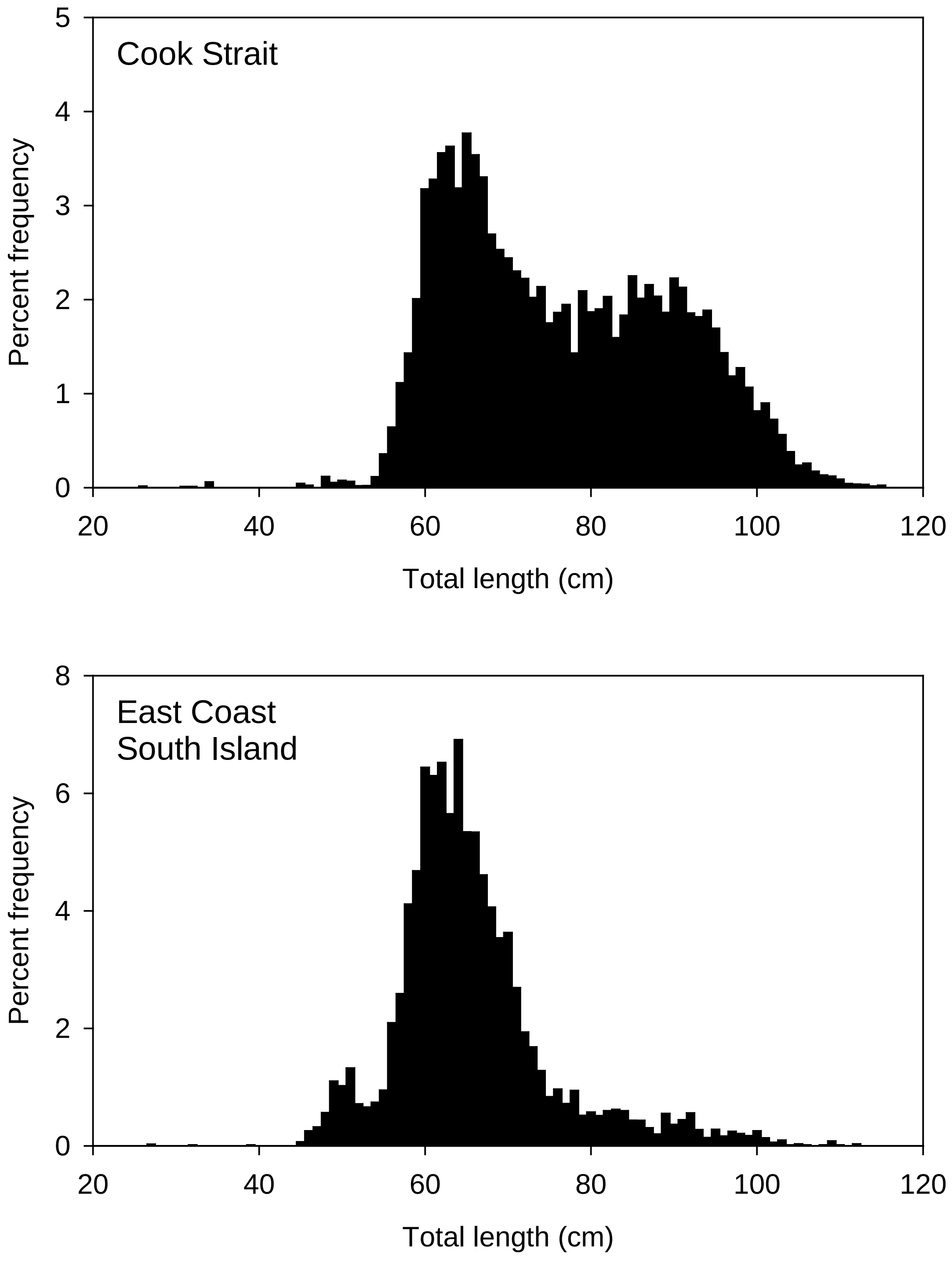

Figure 5: Scaled unsexed length frequency distributions of hoki caught in the commercial fishery in Cook Strait (upper panel) and ECSI (lower panel) in 2019 based on at-sea observer sampling (both areas) and land-based sampling (Cook Strait only). Data were used to estimate the ratios, *r*, of mean weight to mean backscattering cross-section.

Cook Strait

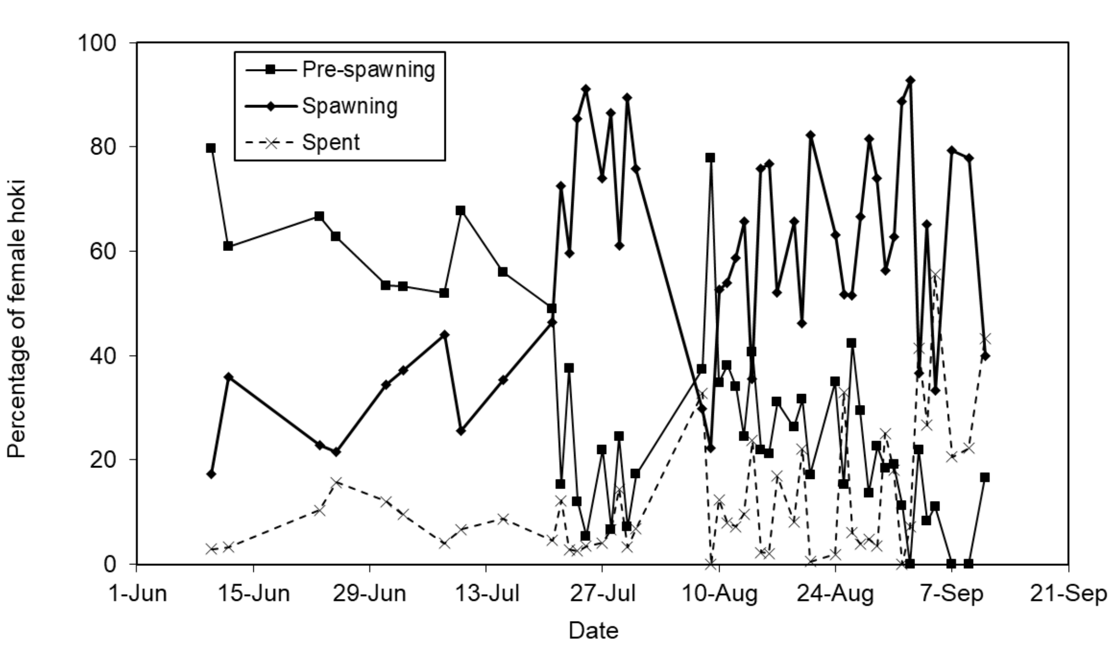

East Coast South Island

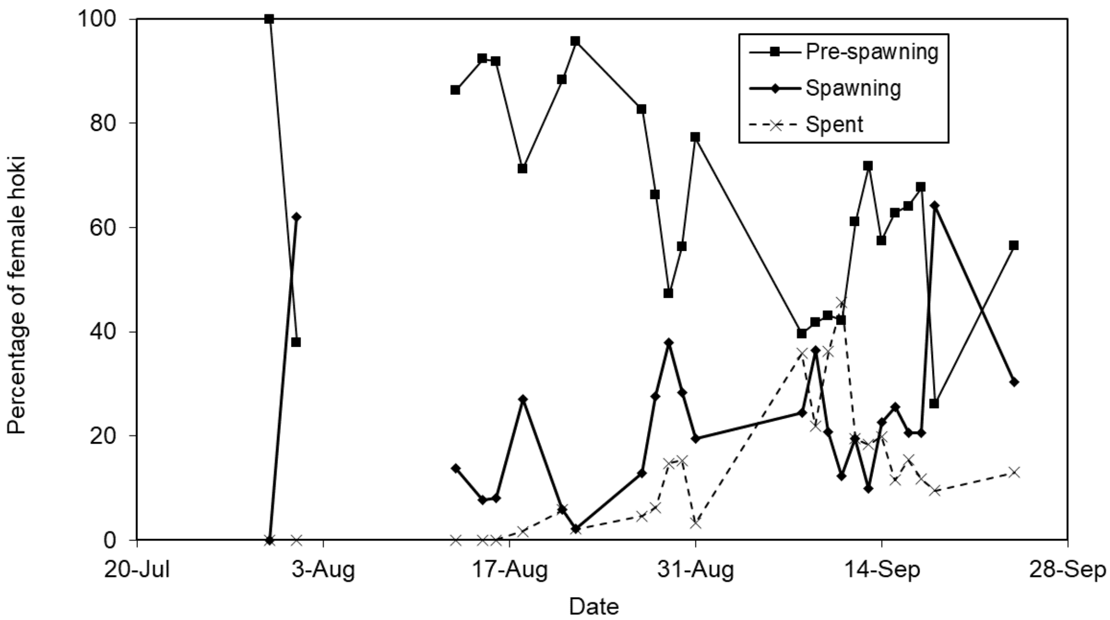

Figure 6: Proportion of female hoki in different maturity states from at-sea observer data and land-based sampling of commercial landings from Cook Strait in 2019 (upper panel) and from observer data from the ECSI in 2019 (lower panel). Research gonad stages are defined in Appendix 2: pre-spawning = gonad stages 1–3 and 6 (observer stages 1 and 2); spawning = gonad stages 4 and 5 (observer stages 3 and 4); post-spawning = gonad stage 7 (observer stage 5). Note that the date range shown are different between the two panels.

Figure 7: Location of trawls (stars) and camera drops (squares) carried out in Cook Strait and ECSI during the 2019 hoki acoustic survey. Station numbers are indicated, and catch details are given in Table 5. Note that where stations are close together not all labels are shown.

Figure 8: Photograph of hoki *in situ* collected during camera drop experiment in Cook Strait (stratum 2) on 6 August.

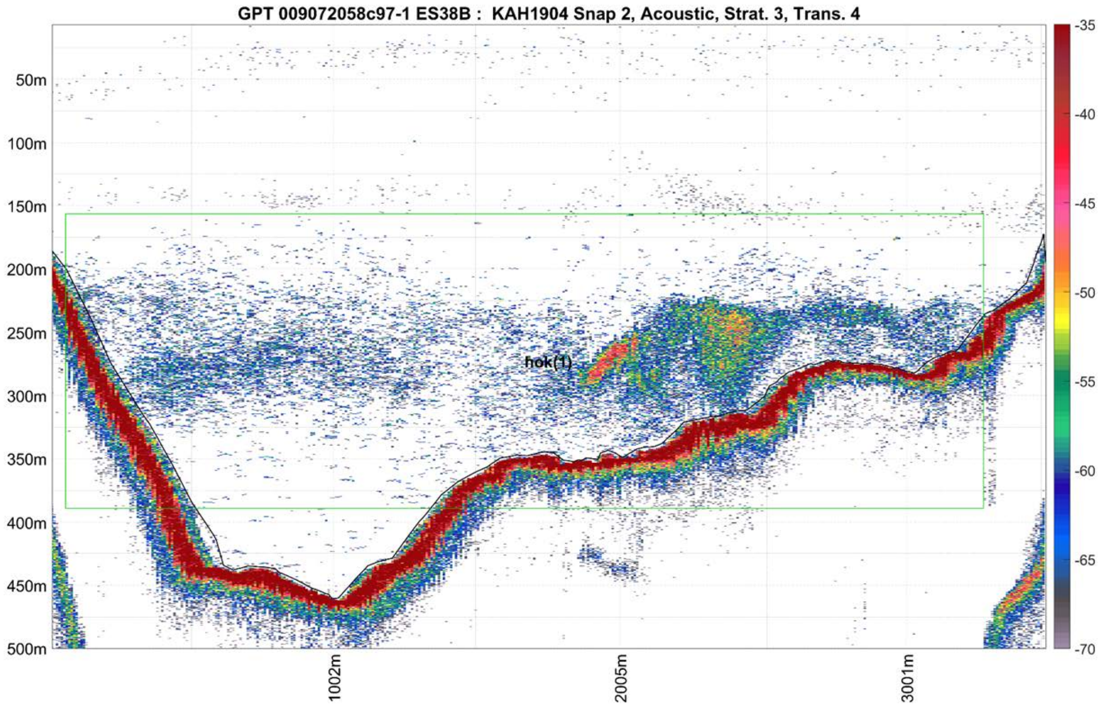

Figure 9: Acoustic echogram from Nicholson Canyon (stratum 3) during snapshot 2 showing a hoki school (‘hok’) from 250-350 m.

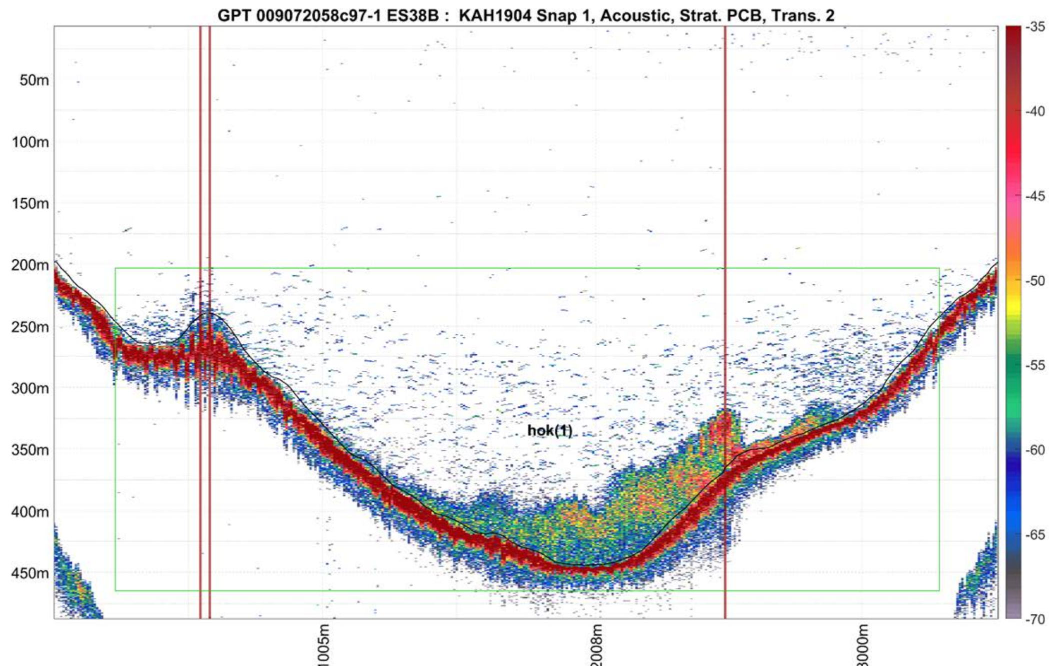

Figure 10: Acoustic echogram from south Pegasus Canyon (stratum PCB) during snapshot 1 showing hoki schools (‘hok’) close to the bottom.

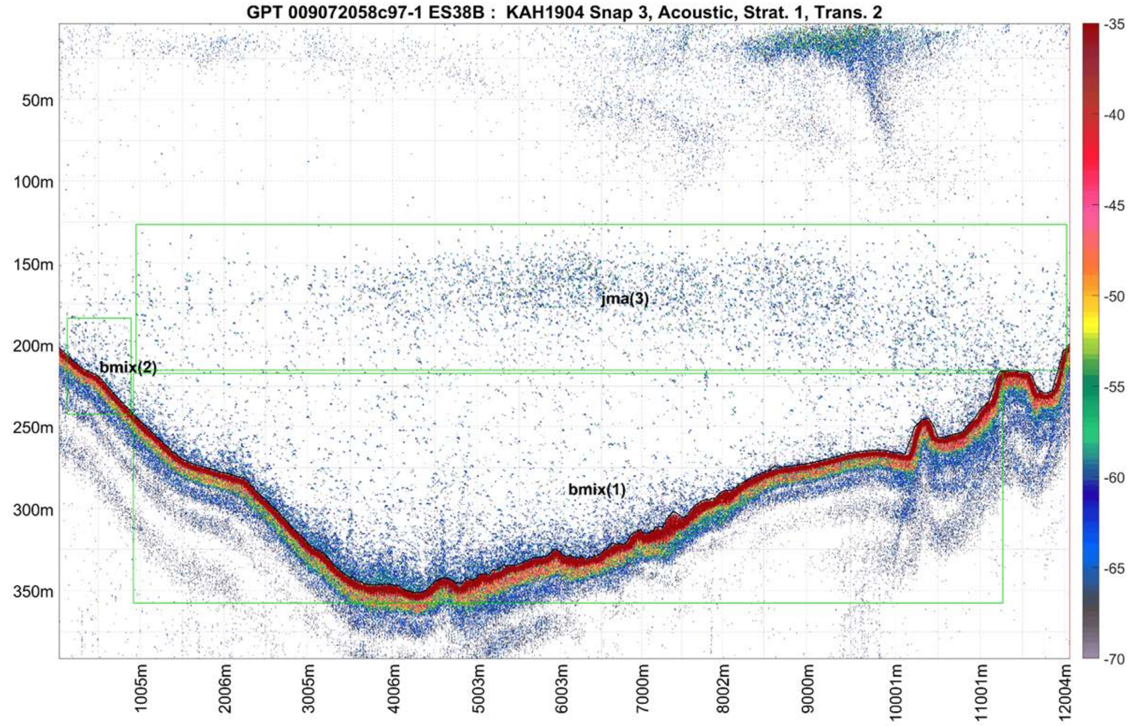

Figure 11: Acoustic echogram from the Narrows Basin (stratum 1) during snapshot 3 showing hoki bottom fuzz ('bmix') marks extending up to 50 m from the bottom. A layer of jack mackerel ('jma') is also defined from 130-210 m.

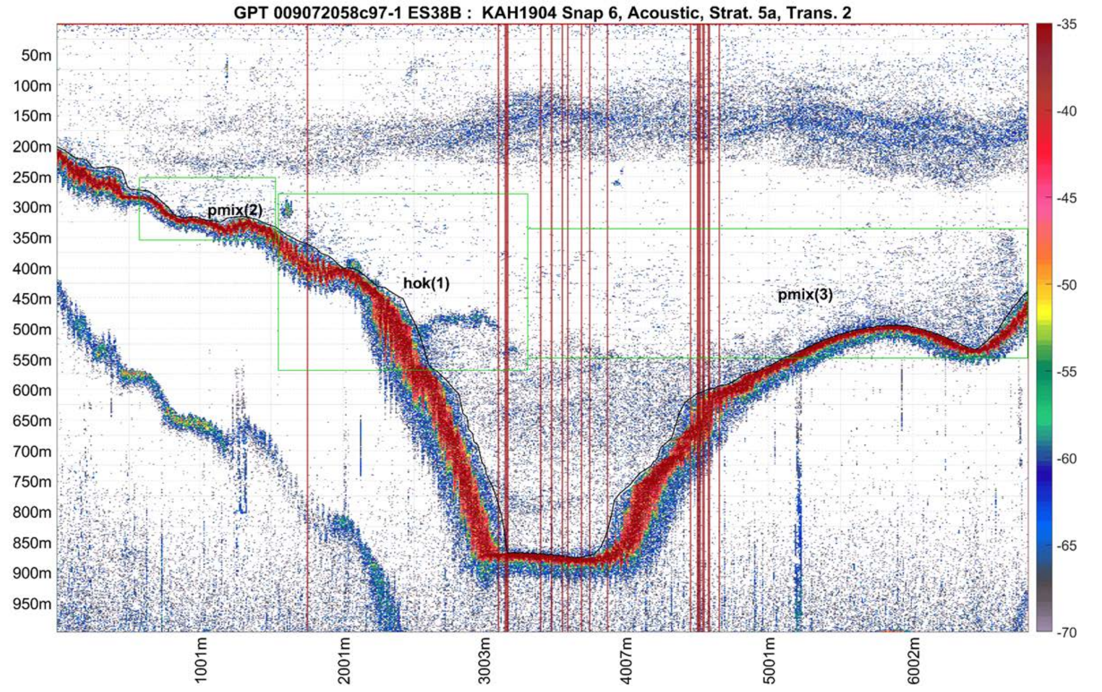

Figure 12: Acoustic echogram from Cook Strait Canyon extension (stratum 5A) during snapshot 6 showing pelagic fuzz ('pmix') marks and a small hoki school ('hok'). Red vertical lines indicate pings that have been excluded due to noise.

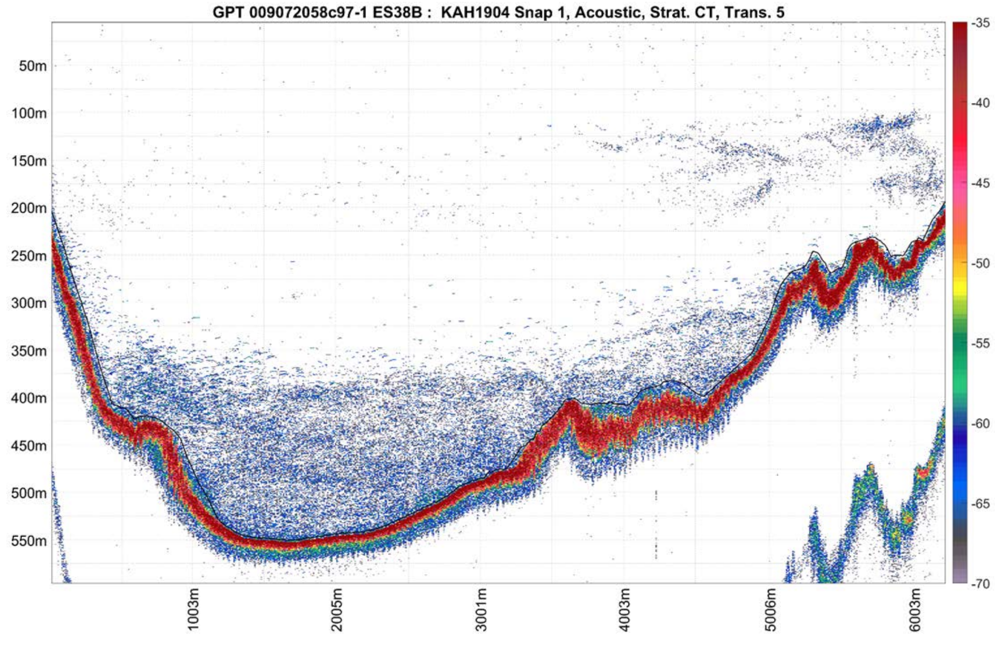

Figure 13: Acoustic echogram from Conway Trough (stratum CT) showing pelagic fuzz deeper than 300 m.

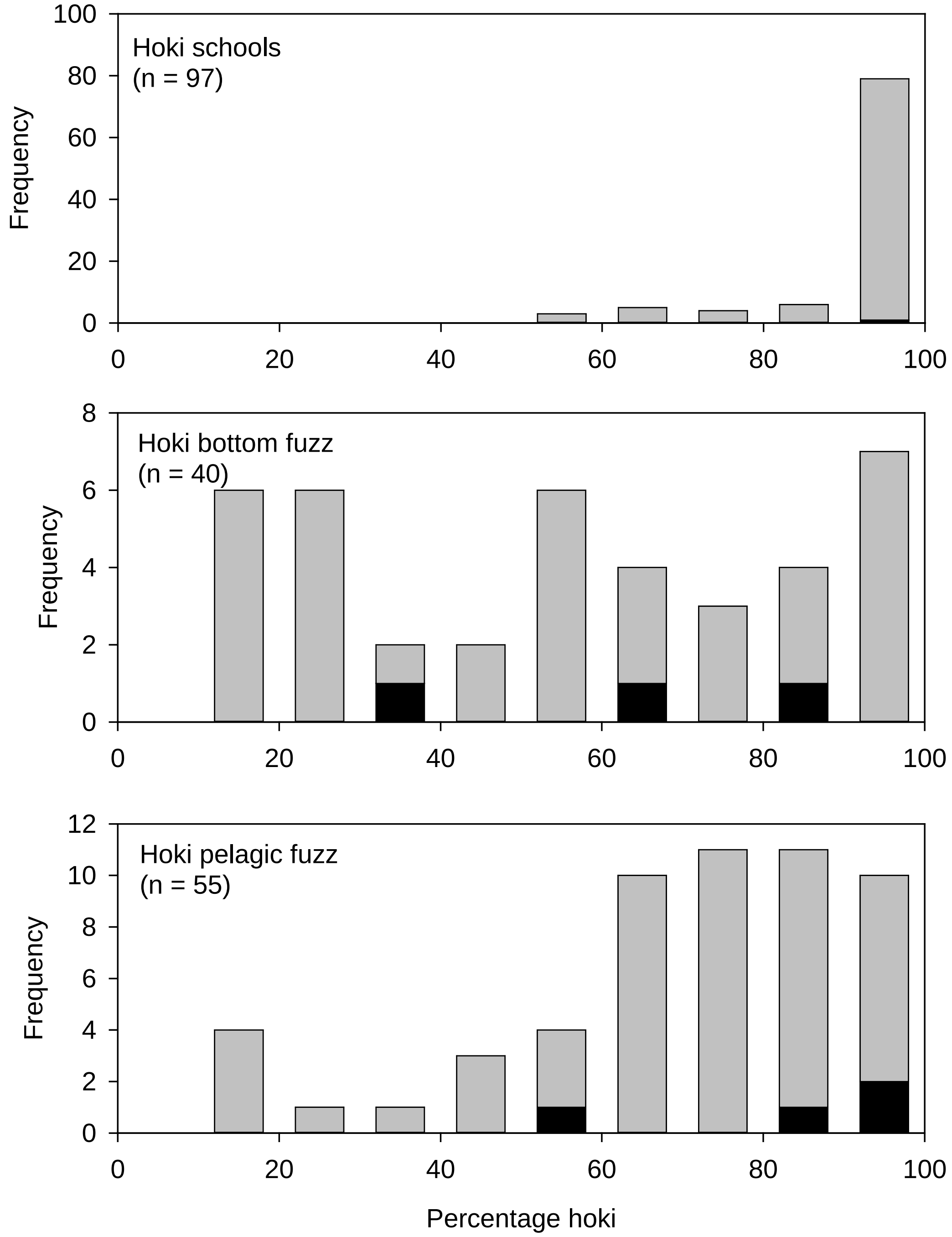

Figure 14: Percentage of hoki by weight in trawls on hoki schools, hoki bottom fuzz, and hoki pelagic fuzz mark types in Cook Strait in 2019 (black bars) compared with trawls on the same mark types in previous Cook Strait surveys in 2001–15 (grey bars). n values refer to the total number of tows (2001–19).

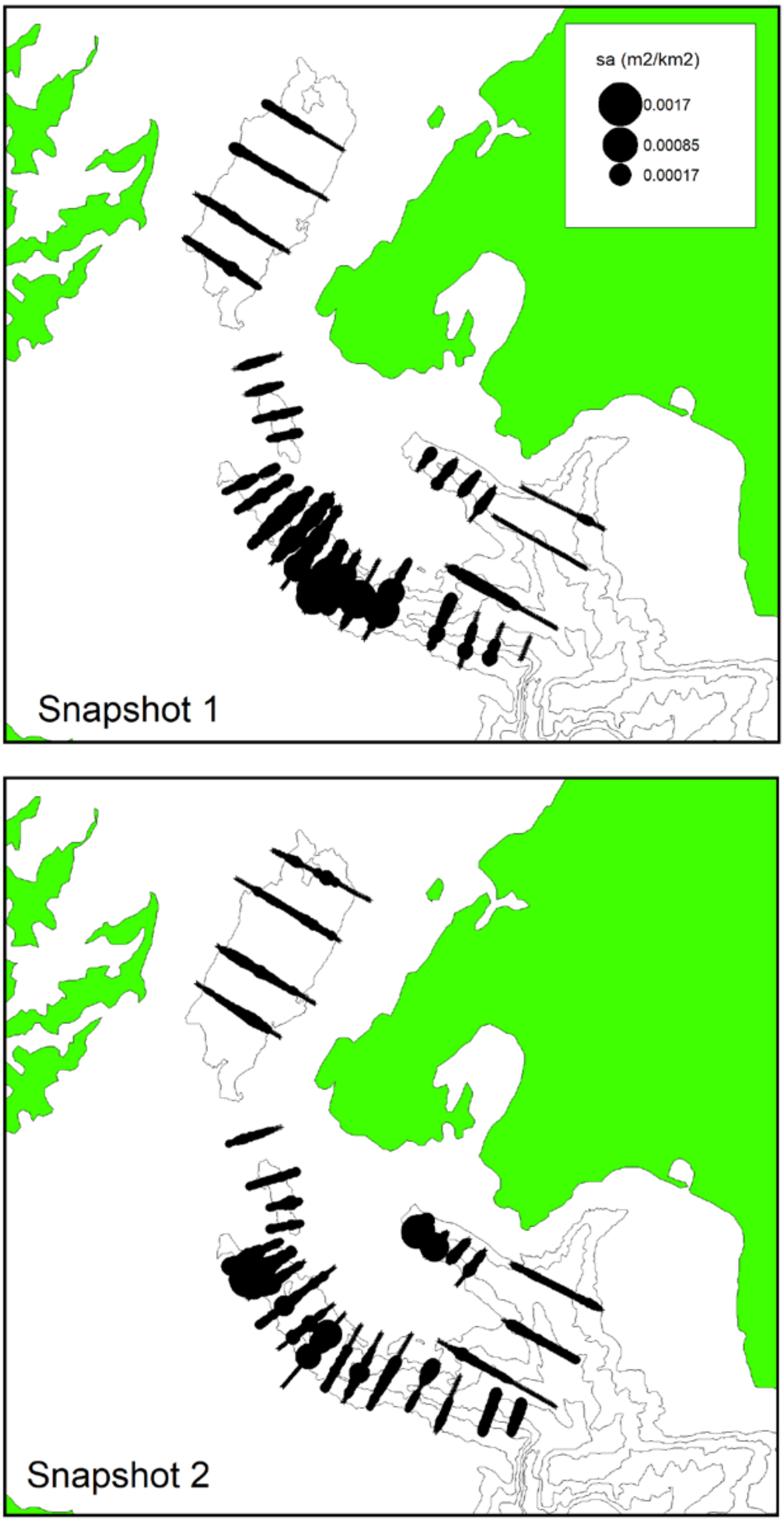

Figure 15: Spatial distribution of hoki acoustic backscatter plotted in 10-ping (~100 m) bins for snapshots 1 and 2 of Cook Strait. Symbol size is proportional to the log of the acoustic backscatter.

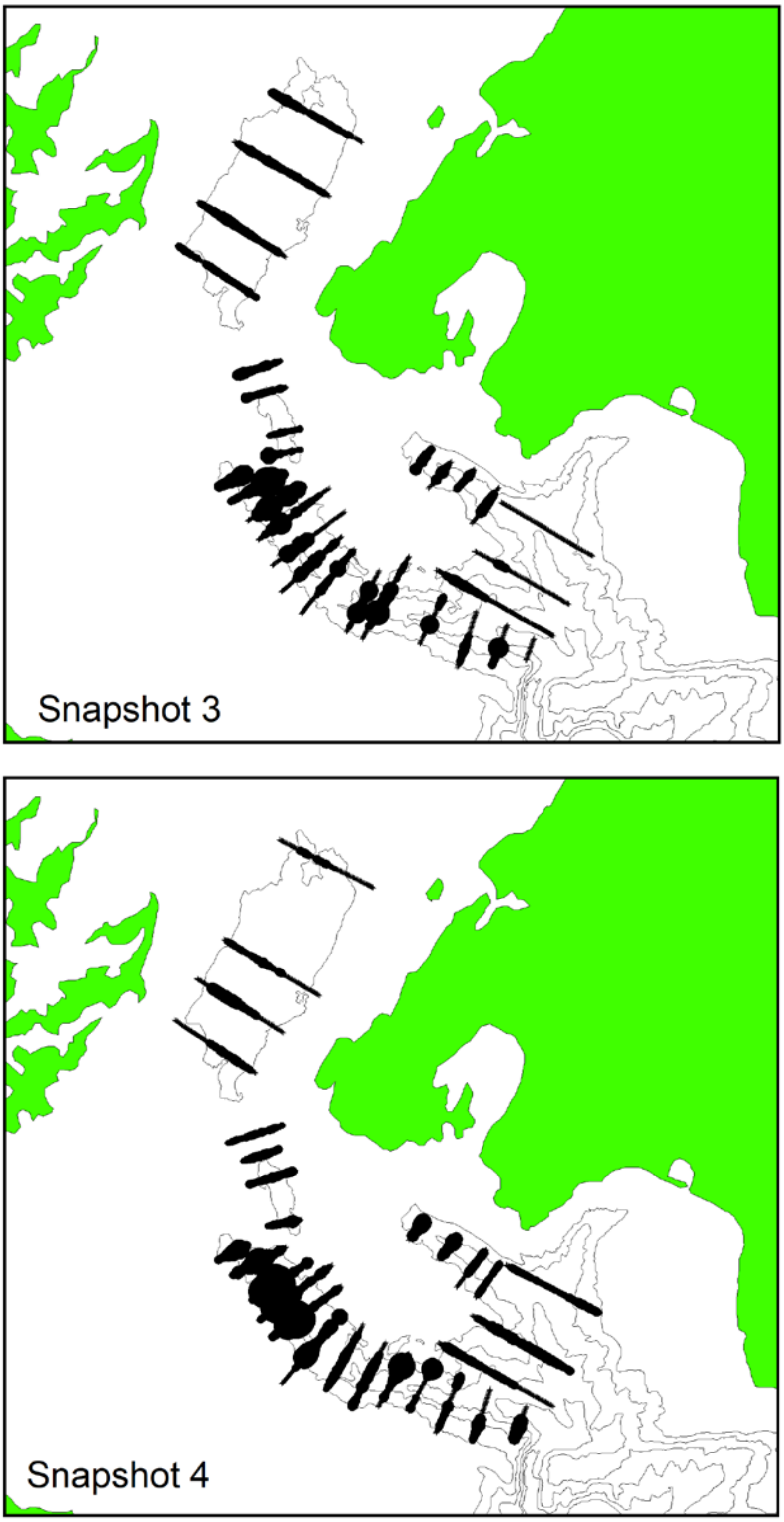

Figure 15 continued: Spatial distribution of hoki acoustic backscatter plotted in 10-ping (~100 m) bins for snapshots 3 and 4 of Cook Strait. Symbol size is proportional to the log of the acoustic backscatter.

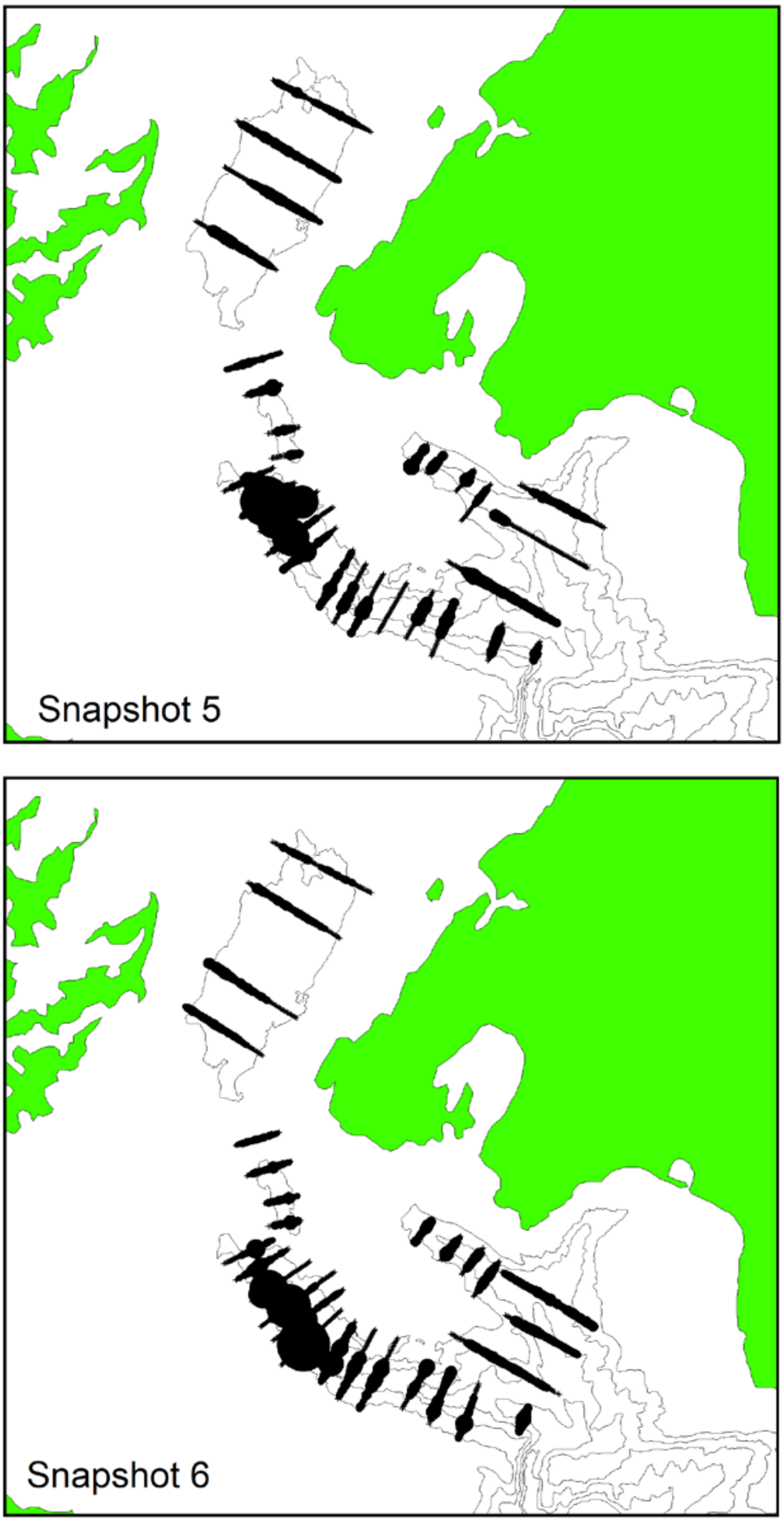

Figure 15 continued: Spatial distribution of hoki acoustic backscatter plotted in 10-ping (~100 m) bins for snapshots 5 and 6 of Cook Strait. Symbol size is proportional to the log of the acoustic backscatter.

Figure 15 continued: Spatial distribution of hoki acoustic backscatter plotted in 10-ping (~100 m) bins for snapshot 7 of Cook Strait. Symbol size is proportional to the log of the acoustic backscatter.

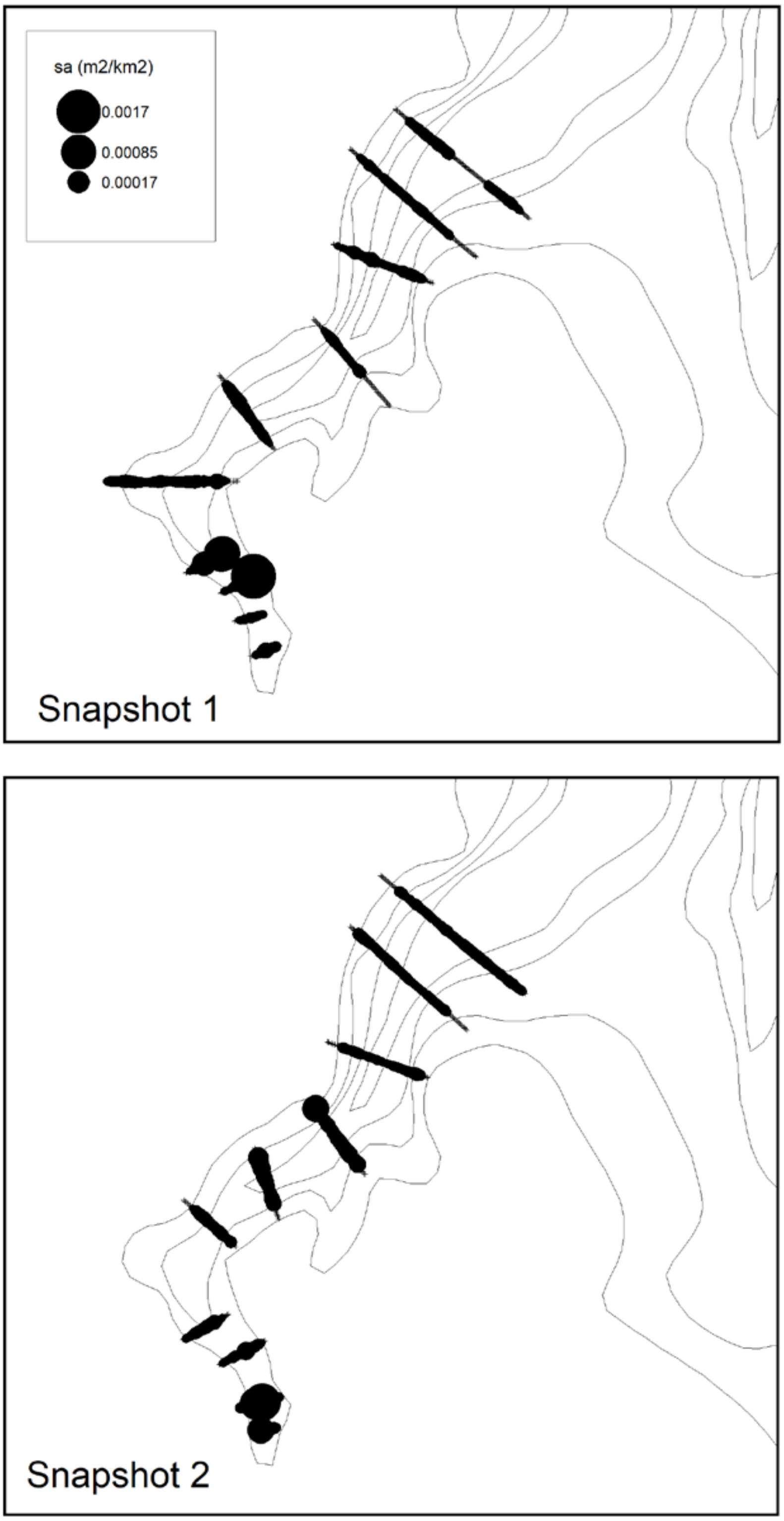

Figure 16: Spatial distribution of hoki acoustic backscatter plotted in 10-ping (~100 m) bins for snapshots 1 and 2 of Pegasus Canyon. Symbol size is proportional to the log of the acoustic backscatter.

Figure 17: Spatial distribution of hoki acoustic backscatter plotted in 10 ping-(~100 m) bins for snapshot of Conway Trough. Symbol size is proportional to the log of the acoustic backscatter.

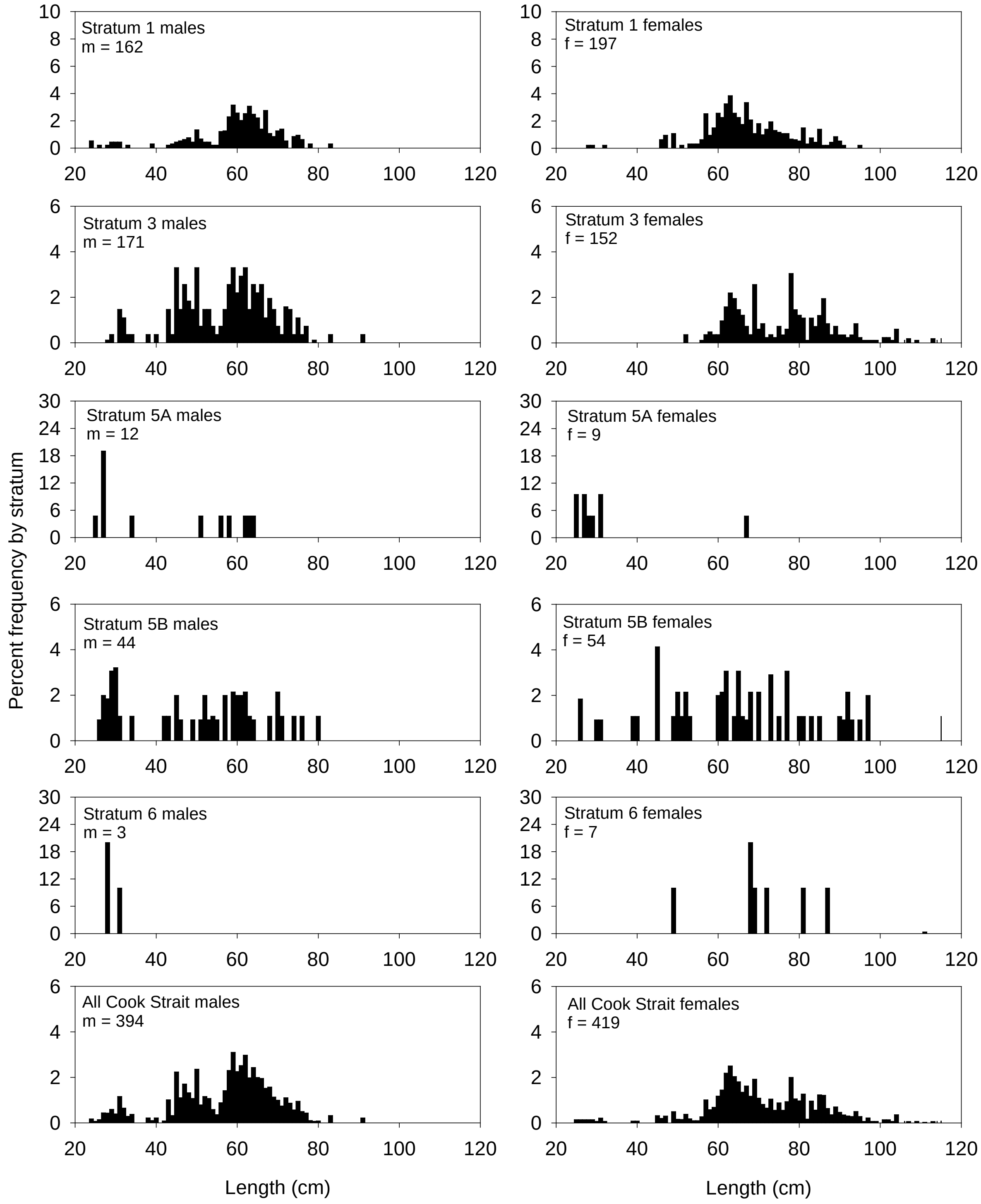

Figure 18: Scaled length frequency distributions of male and female hoki by stratum from research trawls in Cook Strait in winter 2019. Length frequency distributions for each stratum are expressed as a percentage of the total hoki catch in that stratum. m (male) and f (female) values refer to the numbers of fish measured.

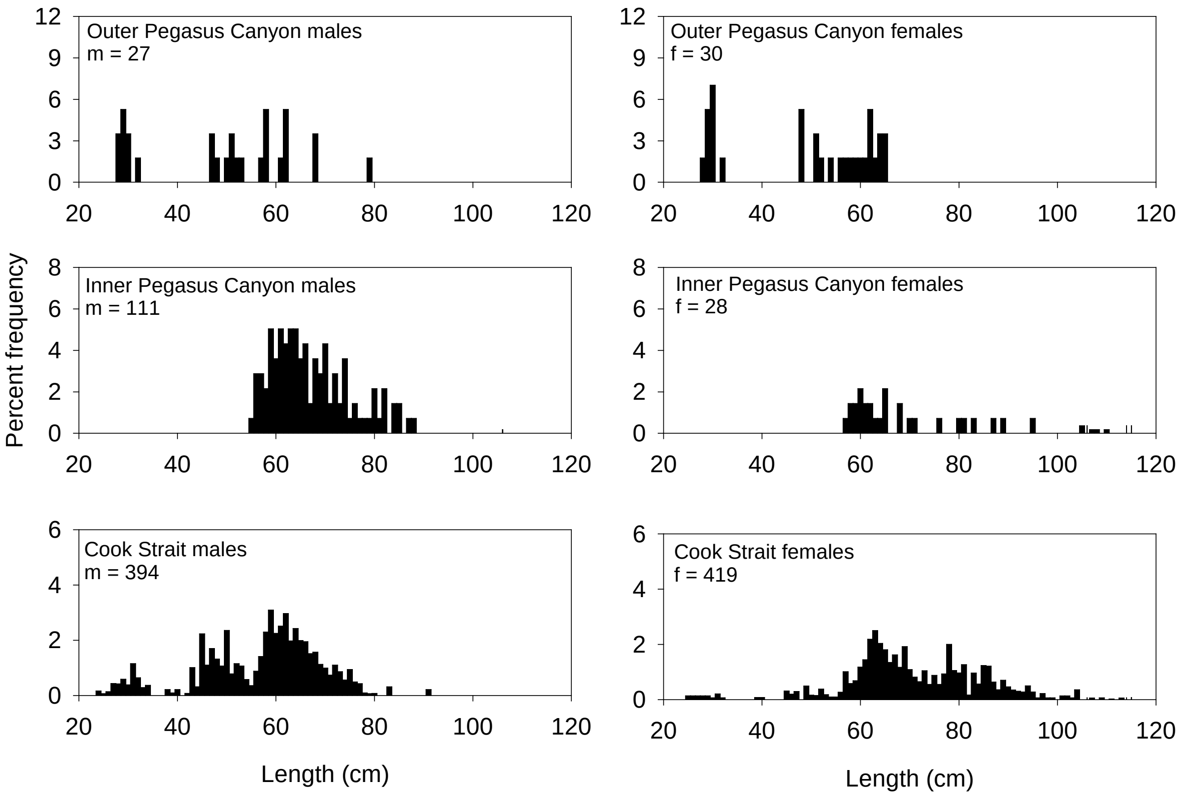

Figure 19: Scaled length frequency distributions of male and female hoki by area from research trawls in Pegasus Canyon in winter 2019 compared with Cook Strait distributions. Length frequency distributions for each area are expressed as a percentage of the total hoki catch in that area. m (male) and f (female) values refer to the numbers of fish measured.

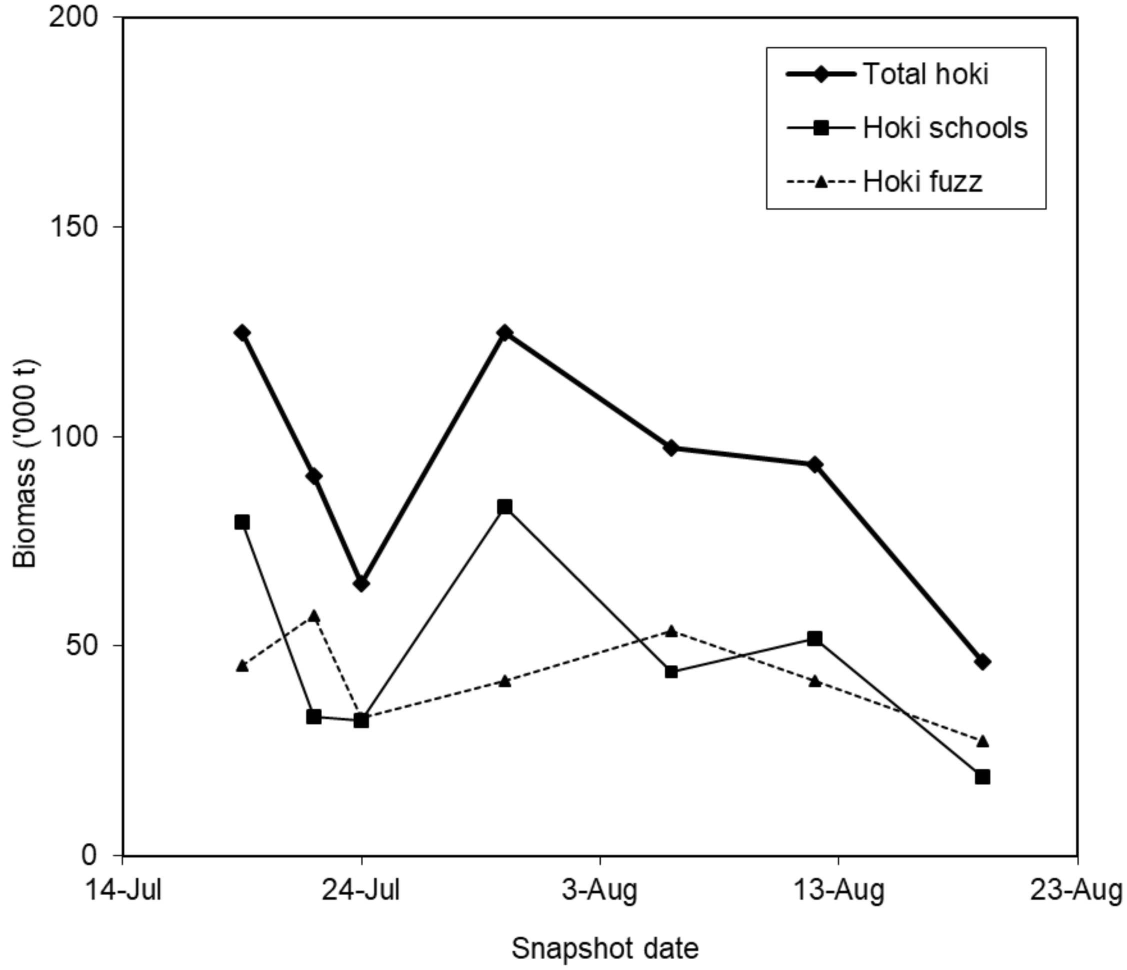

Figure 20: Estimated hoki abundance in Cook Strait by snapshot over the 2019 survey period.

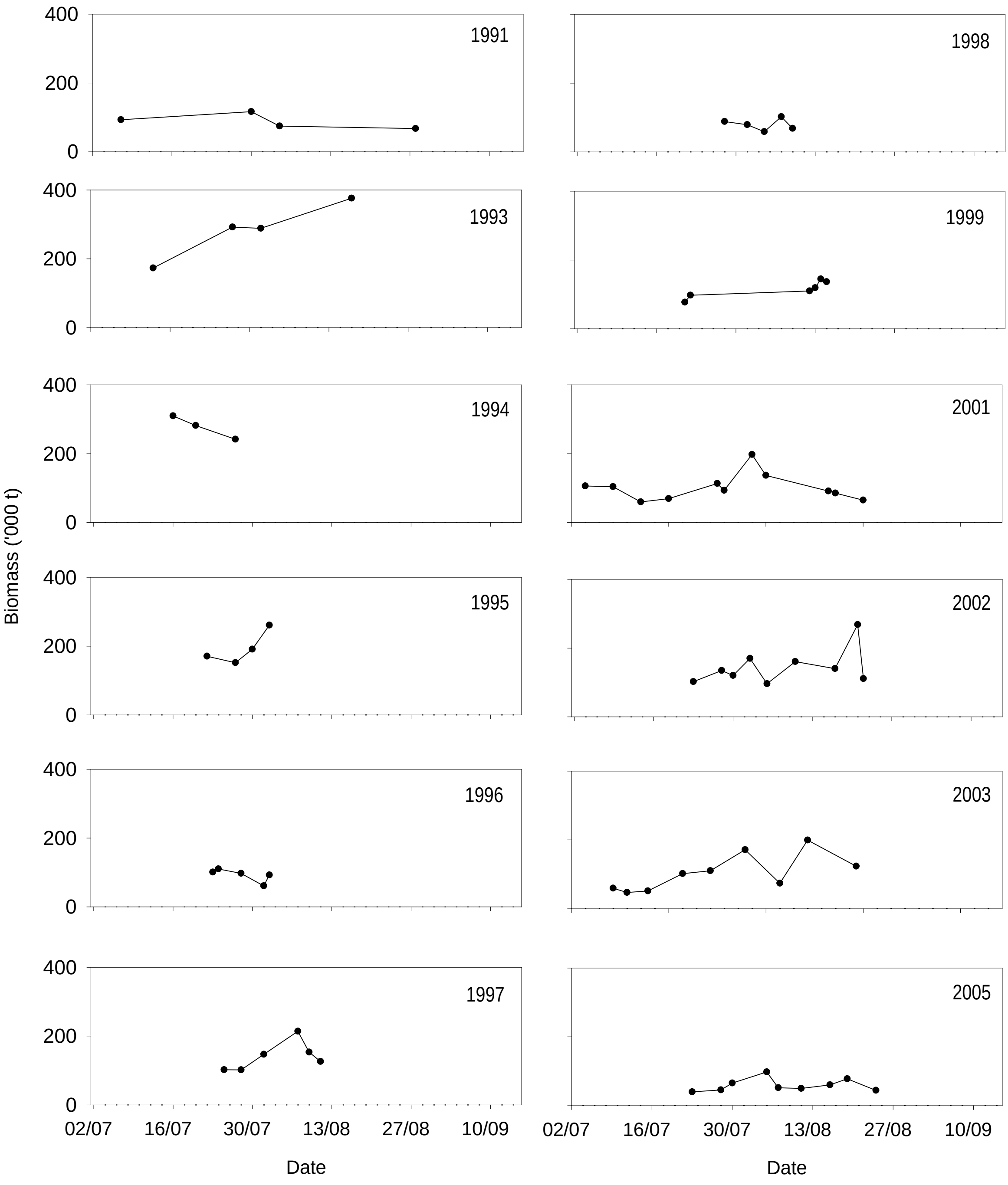

Figure 21: Estimated hoki abundance by snapshot for all acoustic surveys in the Cook Strait time series from 1991-2005.

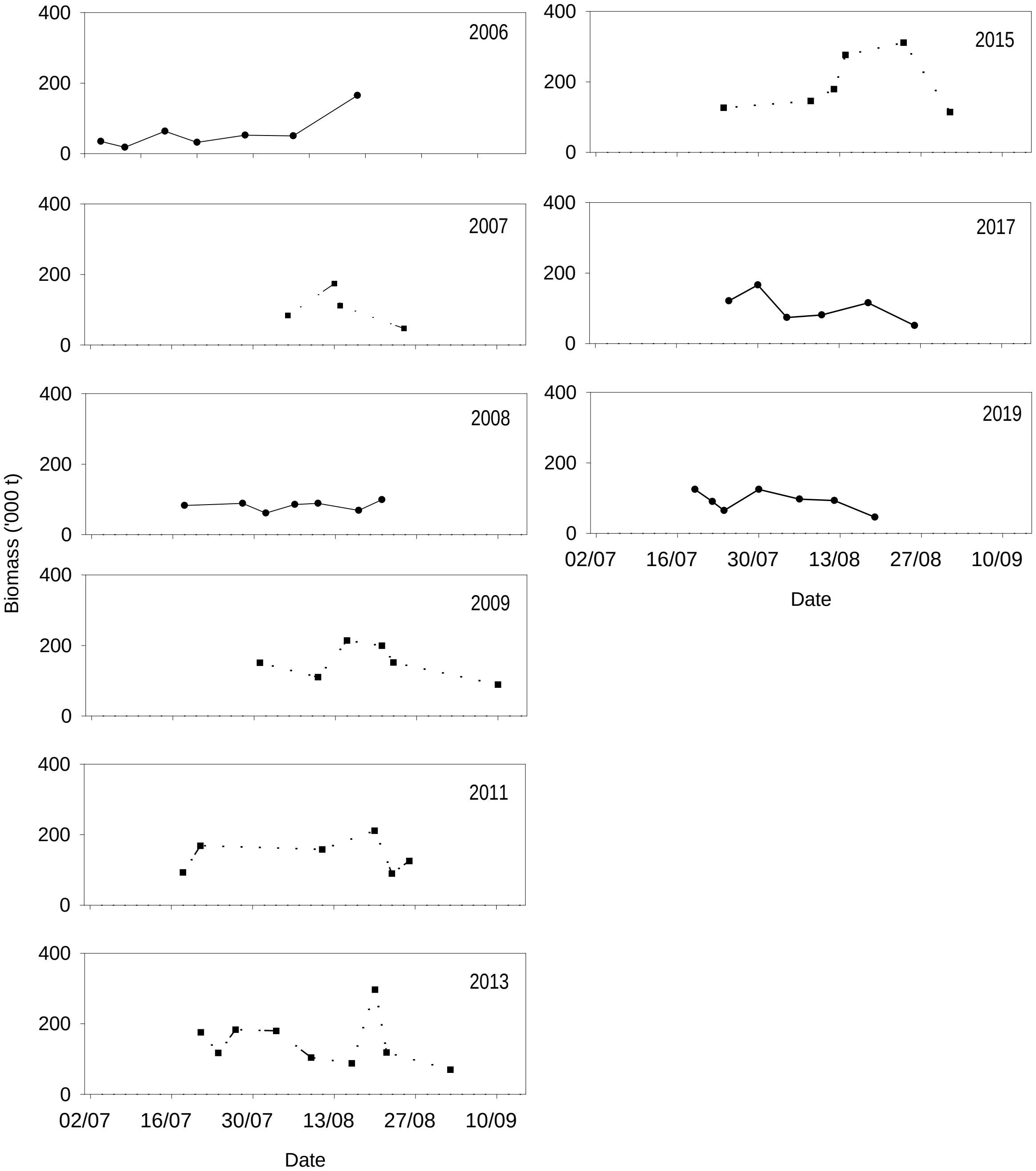

Figure 21 continued: Estimated hoki abundance by snapshot for all acoustic surveys in the Cook Strait time series from 2006-19.

APPENDIX 1: CALIBRATION REPORT *KAHAROA* 18 JULY 2019

An EK60 transceiver was installed on board *Kaharoa* for the Cook Strait hoki survey, as a replacement for the ES60 system normally operated on the vessel. The EK60 was connected to the *Kaharoa*'s 38 kHz hull-mounted Simrad ES38B transducer. Calibration took place in Wellington Harbour, south of Somes Island (41° 15.96' S 174° 51.92' E), on 18 July 2019 at the start of the Cook Strait hoki acoustic survey. Water depth was about 21 m below the transducer. This was the first calibration of the EK60 echosounder on *Kaharoa* since 2008. Previous calibrations of the ES60 echosounder on *Kaharoa* were carried out by NIWA in 2006, 2008, 2013, and 2017, and by CSIRO in 2016.

The calibration was carried out by Pablo Escobar-Flores and Dan MacGibbon following the procedures of Demer et al. (2015). A weighted line was passed under the keel before the vessel was anchored, to facilitate setting up the three calibration braided lines, at the intersection of which the calibration sphere was set. The calibration sphere was suspended below the transducer using a nylon line to minimise the risk of causing variation on the measured target strength due to microbubbles trapped in braided lines. A lead weight was deployed about 3 m below the sphere to steady the arrangement of lines.

The calibration started at 12:25 NZST and was carried at 1.024 ms pulse length and 2000 W power. The weather was good, with northerly winds (15–20 knots) and 0.5 m swell. The sphere was centred in the beam to obtain data for the on-axis calibration and then moved around the beam to obtain data for the beam shape calibration. Calibration was completed at 14:35 NZST.

The calibration data were recorded in one Simrad EK60 raw format file (kah1904-D20190718-T002651.raw) that was stored in the NIWA Fisheries acoustic data repository on the Odin server. The EK60 transceiver settings in effect during the calibration are given in Table A1.1.

Water temperature and salinity measurements were taken using an RBR*concerto* temperature and depth probe, serial number 60314. An estimate of acoustic absorption was calculated using the formulae by Doonan et al. (2003) and an estimate of sound speed was calculated using the formulae by Fofonoff & Millard (1983).

Analysis

The data in the EK60 files were extracted using the software ESP3 (version 1.3.0) (Ladroit 2017). The amplitude of the sphere echoes was obtained by filtering on range and choosing the sample with the highest amplitude. Instances where the sphere echo was disturbed by fish echoes were discarded. The alongship and athwartship beam widths and offsets were calculated by fitting the sphere echo amplitudes to the Simrad theoretical beam pattern:

$$compensation = 6.0206\left(\left(\frac{2\theta_{fa}}{BW_{fa}}\right)^2 + \left(\frac{2\theta_{ps}}{BW_{ps}}\right)^2 - 0.18\left(\frac{2\theta_{fa}}{BW_{fa}}\right)^2\left(\frac{2\theta_{ps}}{BW_{ps}}\right)^2\right),$$

where θ_{ps} is the port/starboard echo angle, θ_{fa} the fore/aft echo angle, BW_{ps} the port/starboard beamwidth, BW_{fa} the fore/aft beamwidth, and *compensation* the value, in dB, to add to an uncompensated echo to yield the compensated echo value. The fitting was done using an unconstrained nonlinear optimisation (as implemented by the Matlab fminsearch function). The Sa correction was calculated from:

$$S_{a,corr} = 5\log_{10}\left(\frac{\sum P_i}{4P_{\max}}\right),$$

where P_i is the sphere echo power measurement and P_{max} the maximum sphere echo power measurement. A value for $S_{a,corr}$ is calculated for all valid sphere echoes and the mean over all sphere echoes is used to determine the final $S_{a,corr}$.

Results and Discussion

The results from the RBR cast are given in Table A1.2, along with estimates of the sphere target strength, sound speed, and acoustic absorption.

The estimated beam pattern and coverage for the calibration are given in Figure A1.1. The two-axes symmetry of the pattern centred on the broad-beam axis indicates that the transducer and EK60 transceiver were operating correctly. The fit between the theoretical beam pattern and the sphere echoes is shown in Figure A1.2 and indicates that the transducer beam pattern is shaped correctly. The RMS of the difference between the Simrad beam model and the sphere echoes out to 3.6º was 0.13 dB (Table A1.3), indicating a calibration of excellent quality (RMS less than 0.2 dB is excellent). G_0 was within the range of values observed and the $S_{a,corr}$ was the same as the one calculated in the 2018 calibration.

Table A1.1: EK60 transceiver settings and other relevant parameters during the calibration.

Parameter	Value
Echosounder	EK60
GPT model/serial	GPT 009072058c97-1
GPT software version	70413
EK80 software version	1.12.2
Transducer model	ES38B
Transducer serial number	30159
Sphere type/size	tungsten carbide/38.1 mm diameter
Operating frequency (kHz)	38
Transducer draft setting (m)	1.0
Transmit power (W)	2000
Pulse length (ms)	1.024
Transducer peak gain (dB)	26.5
Sa correction (dB)	0.0
Bandwidth (Hz)	2425
Sample interval (m)	0.384
Two-way beam angle (dB)	–20.70
Absorption coefficient (dB/km)	9.75
Speed of sound (m/s)	1500
Angle sensitivity (dB) alongship/athwartship	23.0/23.0
3 dB beamwidth (º) alongship/athwartship	7.10/7.10
Angle offset (º) alongship/athwartship	0.0/0.0

Table A1.2: Auxiliary calibration parameters derived from depth and temperature measurements.

Parameter	Value
Mean sphere range (m)	16.4
S.D. of sphere range (m)	0.5
Mean sound speed (m/s)	1494.06
Mean absorption (dB/km)	9.05
Sphere TS (dB re $1m^2$)	–42.40

Table A1.3: Calculated calibration parameters at 1.024 ms using ESP3 from the calibration of the EK60 echosounder in 2019, and results from previous calibrations (although values from 2019 can only be compared to 2006 and 2008, when systems and settings were the same). Transducer peak gain was estimated from mean sphere TS. The 2016 calibration was carried out by CSIRO using a 60 mm copper sphere.

Parameter	2019	2018	2017	2016	2013	2008	2006
Transceiver	EK60	ES60	ES60	ES60	ES60	EK60	EK60
Pulse length (ms)	1.024	1.024	2.048	2.048	2.048	1.024	1.024
Mean TS within 0.21° of centre (dB)	-43.01	-45.00	-44.79		-45.30		
Std dev of TS within 0.21° of centre (dB)	0.16	0.09	0.20		0.40		
Max TS within 0.21° of centre (dB)	-42.64	-44.72	-44.13		-44.82		
No. of echoes within 0.21° of centre	432	315	62	138	75		15
On axis TS from beam-fitting (dB)	-42.86	-44.94	-44.69		-45.45		
Transducer peak gain (mean method) (dB)	25.19	25.21	25.31	25.02	25.05	25.2	25.47
Sa correction (dB)	-0.65	-0.65	-0.43	-0.55	-0.43	-0.71	-0.81
Beamwidth along/athwartship (º)	6.77/ 6.7	7.37/ 7.22	7.0/ 7.2		-	7.1/ 7.1	6.7/ 6.7
Beam offset along/athwartship (º)	-0.04/ -0.06	0.01/ 0.03	0.00/ 0.00		-	-0.05/ 0.00	0.14/ -0.3
RMS deviation (dB)	0.13	0.08	0.11		0.21		
Number of echoes used to estimate beam shape	20 577	15 237	6 418		1 926	19 295	2 841

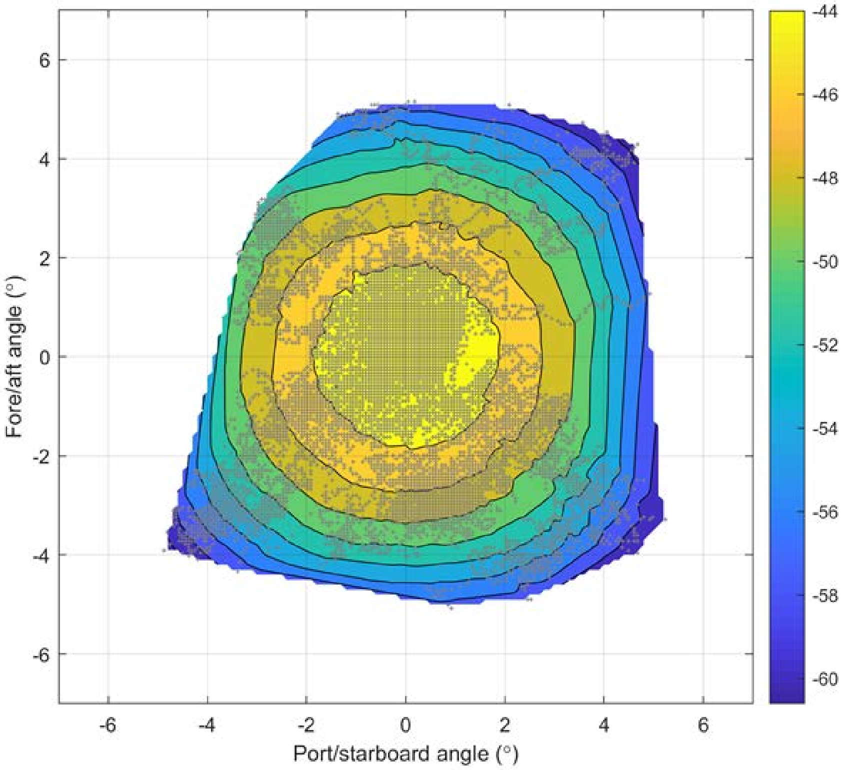

Figure A1.1: The estimated beam pattern from the sphere echo strength and position for the calibration at 1.024 ms pulse length. The '+' symbols indicate where sphere echoes were received. The colours indicate the received sphere echo strength in dB re 1 m^2.

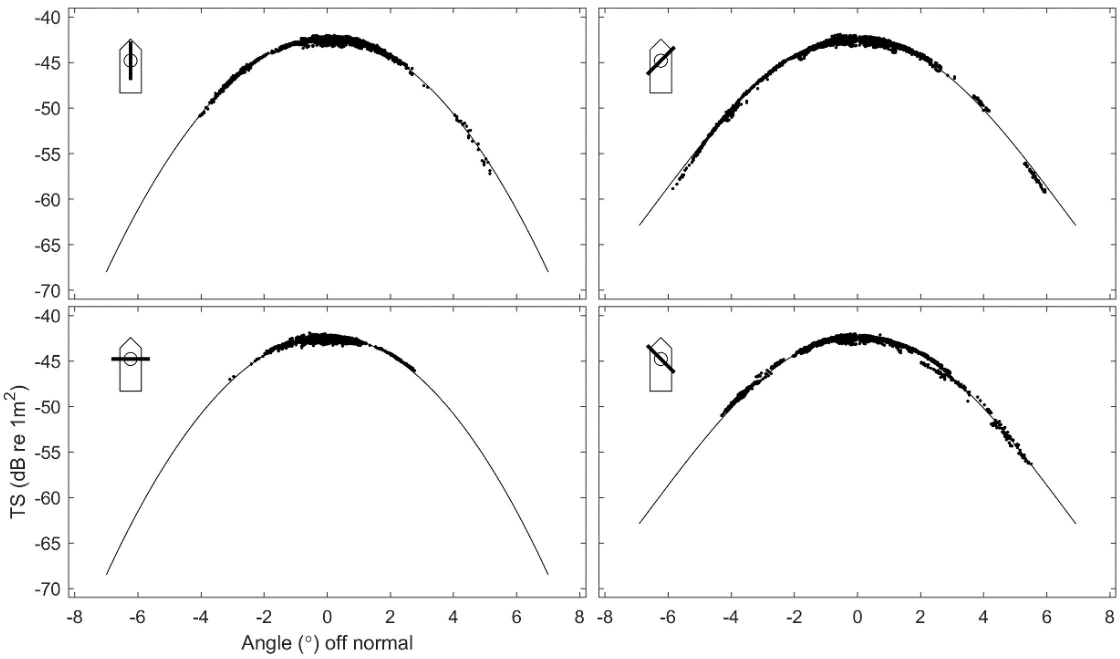

Figure A1.2: Beam pattern results from the calibration at 1.024 ms pulse length. The solid line is the theoretical beam pattern fit to the sphere echoes (points) for four slices through the beam.

APPENDIX 2: DESCRIPTION OF HOKI GONAD STAGES

Research gonad stage		Males	Females
1	Immature	Testes small and translucent, threadlike or narrow membranes.	Ovaries small and translucent. No developing oocytes.
2	Resting	Testes thin and flabby; white or transparent.	Ovaries are developed, but no developing eggs are visible.
3	Ripening	Testes firm and well developed, but no milt is present.	Ovaries contain visible developing eggs, but no hyaline eggs present.
4	Ripe	Testes large, well developed; milt is present and flows when testis is cut, but not when body is squeezed.	Some or all eggs are hyaline, but eggs are not extruded when body is squeezed.
5	Running-ripe	Testis is large, well formed; milt flows easily under pressure on the body.	Eggs flow freely from the ovary when it is cut or the body is pressed.
6	Partially spent	Testis flabby and may be slightly bloodshot, but milt still flows freely under pressure on the body.	Ovary partially deflated, often bloodshot. Some hyaline and ovulated eggs present and flowing from a cut ovary or when the body is squeezed.
7	Spent	Testis is flabby and bloodshot. No milt in most of testis, but there may be some remaining near the lumen. Milt not easily expressed even when present.	Ovary bloodshot; ovary wall may appear thick and white. Some residual ovulated eggs may still remain but will not flow when body is squeezed.